

Synthesis and characterization of Pulsed-Electrodeposited Cr and Cr-ZrO₂ Coating

A THESIS SUBMITTED IN PARTIAL FULFILLMENT OF THE
REQUIREMENTS FOR THE DEGREE OF

**Master of Technology
In**

Metallurgical & Materials Engineering

Submitted
By

**Suprabha Charjren Lakra
Roll No.211MM1200**



**Department of
Metallurgical & Materials Engineering
National Institute of Technology
Rourkela
2012-2013**

Synthesis and characterization of Pulsed-Electrodeposited Cr and Cr-ZrO₂ Coating

A THESIS SUBMITTED IN PARTIAL FULFILLMENT OF THE
REQUIREMENTS FOR THE DEGREE OF

Master of Technology

In

Metallurgical & Materials Engineering

Submitted

By

Suprabha Charjren Lakra

Roll No.211MM1200

Under the guidance of

Prof. A. Basu



**Department of
Metallurgical & Materials Engineering
National Institute of Technology
Rourkela
2012-2013**



**National Institute of Technology
Rourkela**

CERTIFICATE

This is to certify that the thesis entitled, “**SYNTHESIS AND CHARACTERIZATION OF PULSED- ELECTRODEPOSITED Cr AND Cr-ZrO₂ COATING**”, submitted by **Suprabha Charjren Lakra** in partial fulfilment of the requirements for the award of Master of Technology Degree in **Metallurgical and Materials Engineering at the National Institute of Technology, Rourkela** is an authentic work carried out by her under our supervision and guidance.

To the best of our knowledge, the matter embodied in the thesis has not been submitted to any other University/ Institute for the award of any degree or diploma.

Prof. A. Basu

Dept. of Metallurgical and Materials
Engineering

National Institute of Technology

Rourkela-769008

Date:

CONTENTS

<u>Title</u>	<u>page no.</u>
ACKNOWLEDGEMENT	i
LIST OF FIGURES	ii
LIST OF TABLES	iv
ABSTRACT	v
CHAPTER 1	1
INTRODUCTION	2
1.1 Introduction	2
1.2 Objectives and Scope of the present study	3
1.3 Scope of the thesis	3
CHAPTER 2	4
LITERATURE REVIEW	5
2.1 Surface engineering	5
2.2 Surface modifications processes and Techniques	5
2.2.1 Thin film deposition	5
2.2.2 Sputtering Deposition Process	6
2.2.3 Thermal spraying	7
2.2.4 Ion Implantation	8
2.2.5 Macro and Micro Shot Peening	8
2.2.6 Electroplating	9
2.2.7 Electroless plating	9
2.3 Electrodeposition	9
2.3.1 Chromium deposition	10
2.3.2 Factors on which adhesion depends	11
2.3.3 Surface morphology change with following parameters	11
2.4 Pulsed Electrodeposition	13
2.4.1 Type of pulse waveforms	14
2.4.2 Advantages of pulse DC over DC	14
2.4.3 Advantages of pulse deposition technique	15
2.4.6 Technological Applications	15
2.4.5 Disadvantages of PED	16
2.4.4 Significant outcomes of PED	16
2.5 Electrophoreticdeposition	17
2.5.1 Mechanism of electrophoretic deposition	17
2.5.2 Factors influencing EPD	18
2.5.3 Measurement of zeta potential of particles	19
2.6 Electrocodeposition	20
2.6.1 Mechanism of electrolytic co-deposition	21

2.6.2 Effect of electroplating process parameters on co-deposition	23
2.7 Brief Review on Cr composites coating	23
2.8 wear	24
2.8.1 Abrasive Wear	25
2.8.2 Erosive Wear	26
2.8.3 Adhesive Wear	27
2.8.5 Corrosive Wear	27
2.8.4 Surface Fatigue	29
CHAPTER 3	30
EXPERIMENTAL	30
3.1 Sample preparation	30
3.2 Particle size analysis	30
3.3 Plating Solution Preparation	31
3.4 X-ray diffraction studies	32
3.5 Microstructural studies	32
3.5.1 Scanning Electron Microscope (SEM) studies	33
3.6 Surface mechanical property studies	33
3.6.1 Microhardness Measurement	33
3.6.2 Wear Behaviour of the Coatings	34
CHAPTER 4	35
RESULTS AND DISCUSSIONS OF PURE CHROMIUM COATING	35
4.1 XRD analysis	37
4.2 Microstructural analysis	40
4.3 Surface Mechanical properties	41
CHAPTER 5	42
RESULTS AND DISCUSSIONS OF CHROMIUM-ZIRCONIA COATING	42
5.1 Particle Size	42
5.2 Zeta potential Measurement	43
5.3 XRD Analysis	45
5.4 Microstructure Characterization	47
5.5 Microhardness study	49
5.6 wear study	52
CHAPTER 6	52
CONCLUSIONS	53
6.1 Conclusions	53
6.2 Scope of future work	54
CHAPTER 7	55
REFERENCES	56

ACKNOWLEDGEMENT

This thesis is the end of my journey in obtaining my M.Tech. This thesis has been seen through to completion with the support and encouragement of numerous people including my well wishers, my friends and colleagues. I would like to thank all those people who made this thesis possible and a memorable experience for me. It is my pleasure to express my thanks at the end of my thesis to all those who contributed in many ways to the success of this study and made it an unforgettable experience for me.

With deep regards and profound respect, I take this opportunity to express my profound sense of gratitude and indebtedness to **Prof. A. Basu**, Metallurgical and Materials Engineering Department, NIT Rourkela, for introducing the current research topic and for his inspiring supervision, constructive appreciation and valuable suggestion throughout this research work. It would have not been attainable on behalf of me to bring out this thesis without his help and constant encouragement.

I am sincerely thankful to **Dr B. C. Ray**, Professor and Head of Metallurgical and Materials Engineering Department for providing me necessary facility for my work. I express my sincere thanks to **Prof. A. K. Mondal**, the M.Tech Project co-ordinator of Metallurgical and Materials Engineering department. I am also grateful to the Metallurgical and Materials Engineering Dept. of IIT Kharagpur and for different characterization facilities.

I am highly grateful to lab Members of Department of Metallurgical and Materials Engineering, N.I.T., Rourkela, especially **Mr. R. Pattanaik, Mr. S. Hembram, Mr. U.K. Sahu, Mr. Tanti, Mr. Samal, Mr. Pradhan** and **Mr. A.Pal** for their help during the execution of experiments.

Special thanks to my family members, and all my friends of department of Metallurgical and Materials Engineering for being so supportive and helpful in every possible way.

Date:

Suprabha Charjren Lakra

LIST OF FIGURES

FIGURE	DESCRIPTION
Figure 2.1:	Schematic principle of PVD and CVD process: (a) PVD; (b) CVD.
Figure 2.2:	Powder flame spraying process
Figure 2.3:	Demonstration of Shot Peening Process
Figure 2.4:	Major Pulse waveforms for deposition
Figure 2.5:	Schematic diagram of electrical double layer structure and the electric potential near solid surface with stern and Gouy layers (surface charge is assumed to be positive)
Figure 2.6:	pH Vs Zeta potential
Figure 2.7:	Schematic of Electrocodeposition process
Figure 2.8:	Flow chart of various wear mechanisms
Figure 2.9:	Schematic of abrasive wear phenomena
Figure 2.10:	Schematic of fatigue wear, due to the formation of surface and subsurface cracks.
Figure 2.11:	Schematic of erosive wear
Figure 2.12:	Abrasion in the microscale
Figure 3.1:	Nano zeta sizer (Model: Nano ZS, Malvern instrument)
Figure 3.2:	Philips X'pert System
Figure 3.4:	JEOL 6480 LV scanning electron microscope (SEM)
Figure 3.3:	LECO LM700 Michrohardness tester
Figure 4.1:	(a) XRD pattern of Cr coating at different Duty cycle(10,30,50)% at 4 kHz frequency(b) XRD pattern of Cr coating at different frequencies(4,8,12) kHz at duty cycle 10.
Figure 4.2:	SEM image of surface morphology of Cr coatings at different pulse parameters with 350x magnification
Figure 4.3:	SEM image of surface morphology of Cr coatings at different pulse parameters with 1000x magnification
Figure 4.4:	SEM image of surface morphology of Cr coatings at different pulse parameters with 2000x magnification
Figure 4.5:	Sample EDS analysis of the Cr coating.

- Figure 4.6:** Variation of Microhardness with Frequency (i.e. 4, 8, 12 kHz) at Duty cycle (i.e. 10, 30, 50)
- Figure 4.7:** Variation of cumulative depth of wear as a function of sliding distance for the Cr coatings at different plating parameters.
- Figure 4.8:** Wear track of Cr coating (a) without pulse, (b) frequency 4kHz (c) frequency 8kHz(d) frequency 12 kHz and corresponding enlarged view in (e), (f), (g) and (h) respectively.
- Figure 5.1:** Particle size distribution of (a) ZrO_2 powder
- Figure 5.2:** pH Vs Zeta potential for Iso-electric point determination of (a) ZrO_2 .
- Figure 5.3:** (a) XRD pattern of Cr- ZrO_2 at different frequencies(4,8,12)kHz.(b) XRD pattern of Cr- ZrO_2 at different Duty cycle(10,30,50)%.(c) Enlargement of ZrO_2 peaks(8kHz frequency and 30% Duty cycle).
- Figure 5.4:** SEM image of surface morphology of Cr- ZrO_2 Nano-composite coatings at different pulse frequency: (a) no pulse (b) 4 kHz (c) 8 kHz (d) 12 kHz, duty cycle = 50%.
- Figure 5.5:** (a) SEM image of the surface and The corresponding (b) Cr mapping image (c) Zr mapping image, of a Cr- ZrO_2 composite coating produced at frequency of 8 kHz and duty cycle of 30%.
- Figure 5.6:** (a) Effect of pulse frequency and dutycycle on the hardness of Cr- ZrO_2 composite coatings
- Figure 5.7:** Wear depth versus sliding distance plots of Cr- ZrO_2 coatings with different frequencies (4 kHz, 8 kHz, 12 kHz) & different dutycycles (10%, 30%, 50%).
- Figure 5.8:** Wear track of Cr- ZrO_2 coating (a) without pulse, (b) frequency 4kHz (c) frequency 8kHz(d) frequency 12kHz and corresponding enlarged view in (e) ,(f),(g) and(h) respectively.

LIST OF TABLES

- Table 2.1:** Composition of standard bath
- Table 3.1:** Overview of Bath composition and Plating condition
- Table 4.1:** Effect of different frequencies on texture coefficient of Cr coating
- Table 4.2:** Effect of different duty cycle on texture coefficient of Cr coating
- Table 5.1:** Effect of different frequencies on texture coefficient of Cr-ZrO₂ composite coating.
- Table 5.2:** Effect of different duty cycle on texture coefficient of Cr-ZrO₂ composite coating.

ABSTRACT

Chromium is the hardest of the most frequently deposited metals and are used almost exclusively as the final deposit on parts. Without the substantial properties offered by electroplated chromium deposits, the service life of most parts would be much shorter due to wear, corrosion, and the like. Parts would have to be replaced or repaired more often, or they would have to be made from more expensive materials, thus wasting valuable resources. Chromium has special properties, which include resistance to heat, wear, corrosion, erosion and low coefficient of friction. In the present study Chromium (Cr) and chromium – zirconia (Cr-ZrO₂) composite coatings were deposited on low carbon steel substrate by pulse electroplating (PED) technique to enhance tribology and mechanical properties of conventional chromium coating. Zeta potential of ZrO₂ particles in electrolytes was investigated and from the Iso-electric point obtained, the bath pH was maintained at a fixed value. The effect of PED parameter such as frequency and duty cycle on the morphology of the coating was investigated. The structure and morphology of the coating were evaluated using scanning electron microscope (SEM) and x-ray diffraction (XRD). Microhardness tester and ball-on-plate type wear tester were used to access the microhardness and wear resistance of coatings. Finally along with the PED parameters the effect of dispersed ZrO₂ particles on coating properties such as hardness, wear resistance were correlated and it was observed that the change in property was due to dispersion hardening and favourable crystallographic orientations. The crystallite size was averagely 30-50 nm and a strong (220) texture was obtained in composite coatings and in unreinforced Cr coatings a strong (210) texture was determined from the XRD data. The composition and surface morphology of coatings were studied by using EDS and SEM. Hardness and Wear resistance of the coatings were determined by using microhardness tester and ball on plate wear tester, improved hardness and wear resistance of composite coatings were observed compared to the unreinforced chromium coatings. The wear loss behaviour of the coatings developed at different frequency and duty cycle follows the general trend i.e wear loss decreases with increase in frequency and duty cycle. The microhardness values obtained for the composite coatings are higher than the pure Cr coating hardness, the improvement is attributed to dispersion strengthening caused by the embedded second phase particles, texture and modified microstructure of chromium matrix.

Keywords: *Electrodeposition, Electrocodeposition, Chromium, Zirconia, Composite Coating, Wear, Microhardness, Zeta potential.*

CHAPTER 1

INTRODUCTION

Introduction

Objectives and Scope of the Present study

Scope of the thesis

1.1 Introduction

Now-a-days in many industry application such as automobile, aircrafts, biomedical, optical and machinery the main concern is high hardness and wear resistance [1-7]. During metal electroplating the incorporation of inert particles has stimulated scientific and technological interests for decades. This requirement has increase the necessity and development in surface treatments such as coatings using different techniques. There lots of material used for coatings such as copper, nickel, tin, palladium, gold etc. A number of theoretical models have been proposed to describe the electroplating phenomena such as Cr-Co where co-deposition is studied and the results correlated to the requirements for composite co-deposition is reviewed [8]. Cr-MnO₂/TiO₂ where the effects of these dispersed particles are investigated and it is capable of co-deposit with chromium enhances the properties such as hardness, ductility, internal stresses and a high-temperature resistance [9]. Cr-Al₂O₃ co-deposition is achievable when a rare earth element is added into a conventional hexavalent chromium bath. The effect of various plating parameters on Al₂O₃ content of the coating was studied [10]. Cr-MWNT, Chromium-multiwall carbon nanotubes (Cr-MWNT) composite coatings are co-deposited evenly. The introduction of MWNTs evidently enhanced the hardness of Cr coatings [11]. Cr-Al₂O₃/SiC, the co-deposition of the particles and chromium using pulse current, the corrosion behaviour of the composite coating was calculated by potentiodynamic polarization and electrochemical impedance spectroscopy techniques. The result obtained suggested that the Al₂O₃/SiC particles significantly enhanced the corrosion resistance of the composite coating [12]. Cr-WC, Co-deposition had been carried out from a trivalent chromium bath using pulse current. The effect of pulse electroplating Variables such as current density and duty cycle on the amount of incorporated WC particles and morphology of the coatings was investigated [13].

Conversely till date the mechanism of particle co-deposition is not completely understood. This lack of fundamental understanding of the electroplating process has resulted in a trial and error approach being the only method of developing parameters for industrially applicable co-deposition of composite coatings.

In the electrocrystallization process, the structural configuration of electroplated metal and alloy coatings is specified particularly by the interaction between nucleation and crystal

growth [14]. An effective way of controlling these two processes is the use of periodically changing current [15]. In Comparison to convention plating, pulse plating can improve surface appearance and properties, such as smoothness, hardness and enhanced wear resistance in composite coatings [16-21].

1.2 Objectives and Scope of the Present Study

The aim of present study is to improve surface mechanical properties by electro co-deposition of Chromium with dispersed second phase zirconia particles with and without pulse direct current electrodeposition. The objectives can be listed briefly like below:

- Electro co-deposition of Cr with ultra ZrO₂ particle such that the mechanical and electro-chemical properties evenly throughout the surface.
- Characterizations
 - Microstructure and morphology (SEM)
 - Chemical Analysis and phase identification (EDS, XRD)
 - Surface Mechanical properties (Hardness, Wear)
- Optimization of the process
- Correlation with process parameter

1.3 Scope of the thesis

The organization of the rest of the thesis is as follows: The concept of electro co-deposition, their mechanism, applications, parameters for getting better deposition, surface morphology changes with parameters, brief explanation about electrodeposition process with advantages over other coating techniques, applications and about electrocodeposition, effect of different parameters on the properties of electrocodeposited coatings, their applications and brief literature reviews on Cr-ZrO₂ composite coatings were reported in chapter 2. A brief experimental study and different characterization techniques are provided in chapter 3. The characterization of the pure chromium coating with change in mechanical properties by changing the process variables is reported in chapter 4. The study of the different co-deposited samples and the characterization of the coating have been presented in chapter 5. A summary of the main findings along with conclusions is presented in chapter 6. References are provided in Chapter 7.

CHAPTER 2

LITERATURE REVIEW

Surface Engineering

Surface modifications processes and Techniques

Electrodeposition

Pulsed Electrodeposition

Electrophoreticdeposition

Electrocodeposition

Brief Literature Reviews on Cr Nanocomposites

Wear

2.1 Surface engineering

Surface Engineering includes the total field of research and technical activity used for design and is defined as branch of science which deals with the different techniques to achieve desired surface properties and their behaviour in service for engineering components. Surface engineering techniques are being used in the electronic, biomedical, textile, petroleum, petrochemical, automotive, aerospace, missile, power, chemical, cement, machine tools, steel, power, and construction industries [22]. Surface engineering techniques can be used to develop a wide range of functional properties, including electronic, magnetic, electrical, wear-resistant, mechanical and corrosion-resistant properties at the required substrate surfaces.

There are broadly two different categories of surface engineering methods that can be used to enhance the surface properties and the bulk materials. These are surface coatings and surface modification. Surface coating processes involve depositing a layer of molten, semi-molten or chemical material on a substrate surface. One of the main functions of surface coating is to modify and reinforce the surface functions instead of reforming the composition of the bulk material. Some examples of surface coating processes include Chemical Vapour Deposition (CVD), Physical Vapour Deposition (PVD), sol-gel, plasma and thermal spraying, cladding and electroplating [23].

Surface engineering can solve like problems by:

- Implanting alloying atoms to different depths, thereby improving toughness and fatigue properties (surface modification)
- Depositing surface layers, including lubricants (surface coating)
- The surface shape of the component is redesigning to distribute stresses.

2.2 Surface modifications processes and Techniques

There are plentiful commercially available processes and techniques in use for applying coatings to a substrate.

2.2.1 Thin film deposition

Thin film technology is useful in many applications including bio-medical, optics, magnetic, microelectronics, micro-mechanics, sports equipment etc. There are a numerous of deposition methods available. Among them, CVD and PVD are commonly used. For example, the thin

films used today such as flat panel displays, semiconductors, and solar cells are deposited using either PVD or CVD or advanced applications of these processes such as Plasma enhanced CVD (PECVD). Figure 2.1 shows the principle of PVD and CVD processes.

(A) Physical Vapour Deposition (PVD):

In this process vapours are generated either by evaporation from a molten source, or by ejection of atoms from a solid source and is subjected to bombardment by an ionised gas. The vapour may then be left as a stream of neutral atoms in a vacuum or it may be ionised. A partially ionised stream is usually mixed with an ionised gas and then deposited on a substrate, though a highly ionised stream that forms plasma is attracted to the substrate. PVD techniques are limited to making thin films that range from 100 nm to 100 µm [23].

(b) Chemical Vapour Deposition (CVD):

In this process a chemical reaction between the source gases takes place in a chamber. As a result a solid phase material is formed and condensed on the substrate surfaces. In any CVD reaction, it follows three steps:

- A volatile carrier compound is produced from the reaction, e.g. nickel carbonyl.
- Without decomposition, the gas is transport to the deposition site.
- To produce the coating on the substrate a chemical reaction necessary.

CVD is used for both thin films and for coatings in excess of 1 mm [23]. The CVD process has been applied to the deposition of diamond-like films. CVD has a broad use in applying thin films of TiN and TiC on metal working and forming tools and on components that are subject to abrasion and corrosion.

2.2.2 Sputtering Deposition Process:

Sputtering is a process where coating on a material is done by dislodging and ejecting from a solid surface caused by bombardment of high energy particles. The high energy particles are typically positive ions of a heavy inert gas or species of coating material. The sputtered material is ejected primarily in atomic form from the source of the coating material, called the target. The substrate is sited in front of the target so the flux of sputtered atoms is intercepted. The basic processes involving sputtering are ion beam and glow discharge.

A wide range of metal oxides, carbides, and nitrides can be deposited by sputtering. E.g. TiN, TiC, DLC, TiAlN, MoS₂, CrN, Sputtering is a line of site deposition technique.

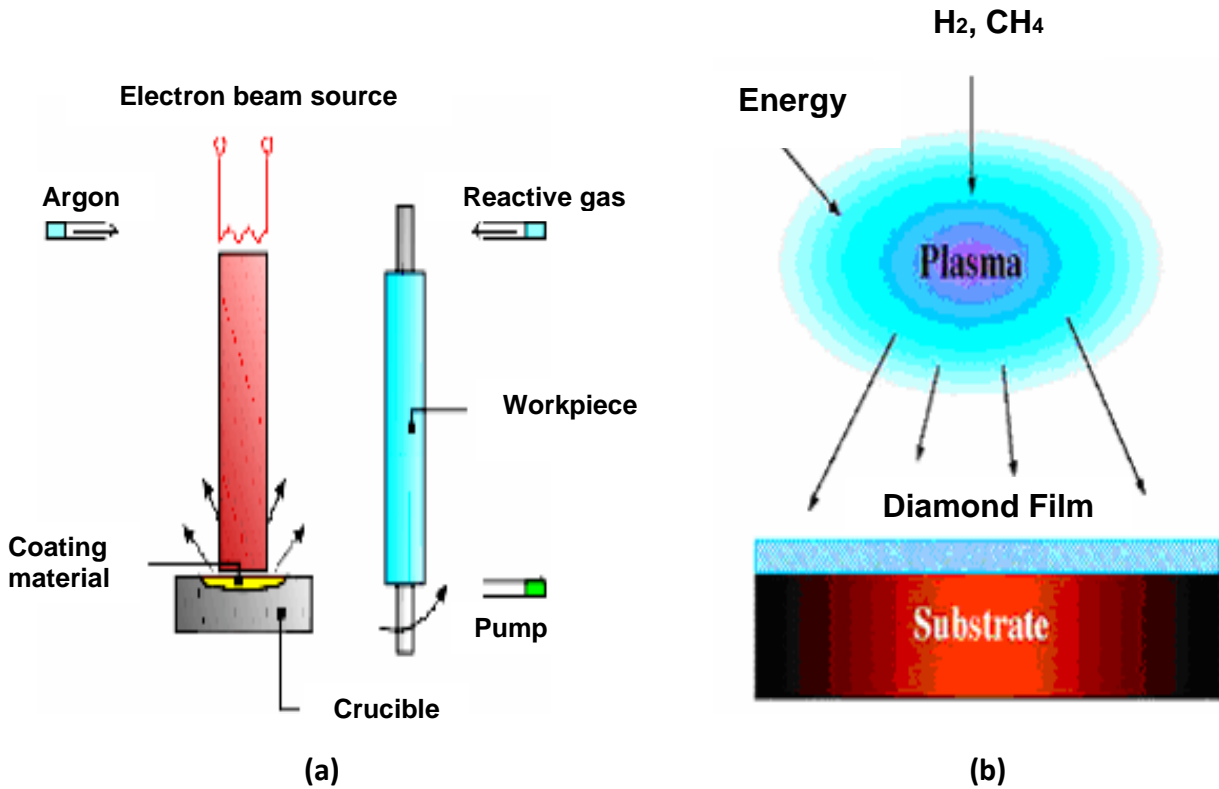


Figure 2.1: Schematic principle of PVD and CVD process: (a) PVD (b) CVD [80].

2.2.3 Thermal spraying:

It is one of the most versatile techniques available for the application of protective coatings. Metals, ceramics and polymers are the most extensively used coating materials. Flame spraying is the simplest method which has two forms of consumables available for use – powder and wire. An example of a typical powder flame spray process is shown in figure 2.2.

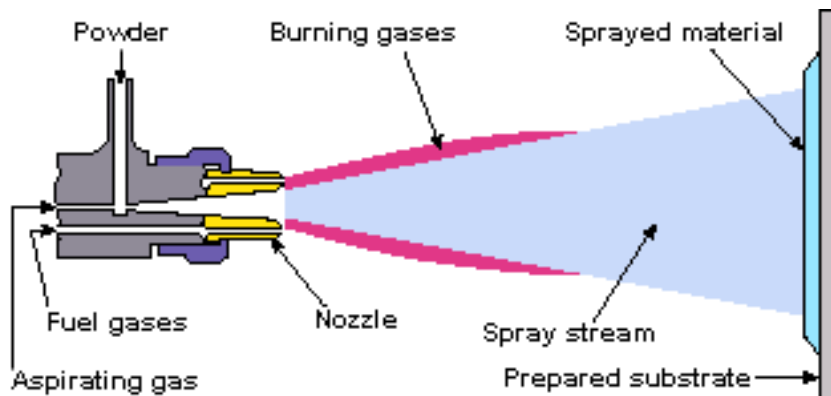


Figure 2.2: Powder flame spraying process [81].

2.2.4 Ion Implantation:

It is the surface modification process where ions are injected into the surface region of a substrate. These processes can enhance properties of substrate material properties such as wear resistance, corrosion resistance, hardness and fatigue, thus improving the service life of the product. Moreover, it is a potential improvement method for plating processes, such as chrome plating. High-energy ions, usually 10–200 keV in energy, are produced, accelerated and directed as a beam onto the surface of the substrate.

The modern method of implantation is plasma source ion implantation. This type of ion implantation involves using plasma as a source which was excited from a gas typically through the use of an RF antenna. Ion implantation processes commonly have products like borides, carbides and nitrides, etc.

2.2.5 Macro and Micro Shot Peening:

It is a modification process where of the surface of a part is cold formed. A stream shot of round hardened steel or similar is propelled to the surface during the process. The general process of shot peening is shown in Figure 2.3. This is nonabrasive and improves the fatigue properties of the part by the introducing compression stresses in the surface layer. The presence compressive stress on this surface serves to retard the initiation and growth of fatigue cracks. This process can be conducted on a macro or micro scale, depending on the mechanism and applications. Shot size is usually of the order of 10 mm diameter and is used in large operations such as on Airbus wheels and micro shot, the order 4 to 50 micron diameter can be used to improve the properties of thin films. Other parts that are usually shot peened include rudders, axles, torsion bars, marine propellers, and exhaust megaphones.

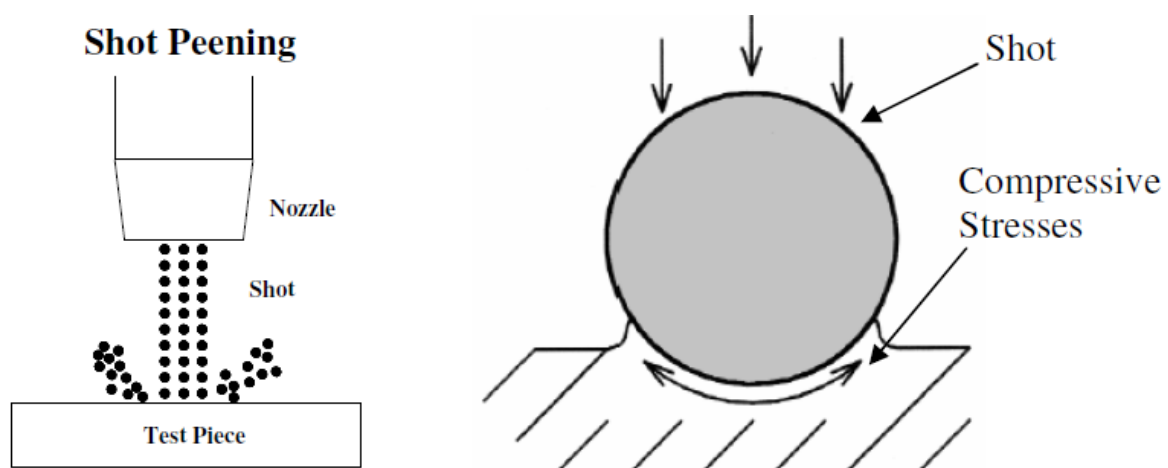


Figure 2.3: Demonstration of Shot Peening Process [82].

2.2.6 Electroplating:

Electroplating is often also called "electrodeposition", it is a process of coating, deposition on a cathode part immersed into an electrolyte solution, where the material of anode is dissolved into the solution in form of the metal ions, travelling through the solution and depositing on the cathode surface. It's a process using electrical current to reduce cations of a desired material from a solution and coat that material as a thin film onto a conductive substrate surface.

2.2.7 Electroless plating:

It is a process which involves no external current to reduce the metal cations into metal atoms rather metal coatings in this process are produced by chemical reduction with electrons supplied by a reducing agent (R.A.) present in the solution. The process was reported by Brenner and Riddell [24] in 1946 for nickel and cobalt coatings and has been using extension to electroless plating of, platinum, silver, copper, gold, palladium and a variety of alloys involving one or more of these metals.

2.3 Electrodeposition:

Electroplating is often also called "electrodeposition", it is a process of deposition on a cathode part immersed into an electrolyte solution, where the material of anode is dissolved into the solution in form of the metal ions, travelling through the solution and depositing on the cathode surface. It's a process using electrical current to reduce cations of a desired material from a solution and coat that material as a thin film onto a conductive substrate surface. Bath composition, *pH*, temperature, type of power supply, current density are the key parameters which influences the deposition process and hence the properties of the deposited materials. it is used immensely due to its certain advantages over other as it is of low energy requirement, low cost, simple scale-up, capability to handle complex geometry, with easily maintain equipment, easily maintained equipment, good chemical stability, and after all very important potential of it is a very large number of pure metals, ceramics, alloys, composites which can be electrodeposited with grain size less than 100 nm [25]. In this process Metals, alloys and polymers can be deposited such as Ni, Cu, Zn, Cr, Co, Au etc [27-30]. A number of theoretical models have been proposed to describe the electroplating phenomena such as Cr-Co, Cr-MnO₂/TiO₂, Cr-Al₂O₃, Cr-MWNT, Cr-Al₂O₃/SiC, Cr-WC, Co-Cu, Ni-Co[8-13, 31-32]. The coating materials are used for large applications as coatings of engine cylinders, musical instruments, high pressure valves, car accessories, aerospace, small aircraft

microelectronics, medical devices, agriculture, marine, and nuclear fields. Polystyrene, PTFE, rubbers, perplex, are the polymer materials used for coating in industrial application [33-37].

2.3.1 Chromium deposition

The commercial process of chromium plating resulted largely from the work of C. G. Fink and C. H. Eldridge, in 1923 and 1924. The hard chrome process using the standard chromic-sulfate bath was in commercial use around 1930 [38-40]. Chromium is the hardest of the most frequently deposited metals and are used almost exclusively as the final deposit on parts. Chromium has special properties, which include resistance to heat, wear, corrosion, erosion and low coefficient of friction [8-13, 41-42]. Chromium plating, therefore, is broadly used as a final finishing process. Deposition of chromium falls in two categories: Decorative, where thin coatings deposit have thickness are usually less than 0.80 μm serve as a non-tarnishing, industrial, and durable surface finish or "Hard" chromium, where thick coatings deposits have a thickness usually greater than 0.80 μm to take advantage of the special properties of chromium, which include resistance to corrosion, erosion, heat, wear, low coefficient of friction and anti galling.

Decorative chromium deposits are used on such items as household appliances, automobile bumpers and trim, furniture and many other articles that require a bright and aesthetic appearance. Our concern for the rest of this report, however, will be with hard chrome plating. Hard chrome is used as a wear resistant coating not only on steel but also on a wide variety of other metals. The electro-deposition of hard chrome is a known means of prolong life of all types of metal parts subjected to wear, abrasion, friction, and corrosion.

Hard chromium because of its low surface energy is more regularly deposited on sliding or revolving parts and is therefore used on hydraulic and pneumatic rods, engines, pumps, compressors etc. The hard chromium deposit is also extremely resistant to corrosion and a large number of applications where it is used to protect parts from corrosion. Ceramic particles deposition on metal substrate can be used to improve the mechanical properties of substrate such as wear resistance, hardness, corrosion, protection against high temperature and oxidation [8-13].

In chromium electroplating method, stainless steel plate is used as anode and the material to be plated used as cathode. The Direct current to the anode is oxidizing the metal atoms and allows them to dissolve in the solution. The dissolved Chromium ions in the electrolyte solution travelling through the solution and get deposited on the cathode.

Table 2.1: Composition of standard bath

Electrolytes	Chromic acid (Cr ₂ O ₃)= 250 g/l
	Sulphuric acid (H ₂ SO ₄)= 2.5 g/l
Conditions	Temperature: 47±2 ° C
	Cathode current density: 7 mA/mm ²

2.3.2 Factors on which adhesion depends

- **Substrate:** The substrate may be metal, alloying elements of different types of steels and copper alloys. Most commercially existing metals are polycrystalline and multiphase system.
- **Cleanliness of the surface:** The satisfactory adhesion of chromium deposits, the surface must be almost perfectly clean and free from any grease. Therefore the substrate surface prior to the coating operation is given cleaning treatments in order to ensure strong and uniform adhesion of the coating to the substrate. Mechanical removal of burrs, solid particles, scales and oxides from the surface is done by abrasion, vibratory finishing, and blast finishing or shot peening [34].
- **Heterogeneity of the surface:** Surface defects and imperfection are the two main cause of heterogeneity [34]. The defect sites have high energy linked in as comparison to other sites of the same surface which leads in variation of heats of absorption or entropy with variation of surface energy. If these heterogeneous samples are to be prepared for deposition, they are highly worked or deformed which involves grinding, machining, polishing.
- **Effect of temperature:** The adsorption phenomenon differs from general under the chemisorptions as activation energy concept is associated with this process [34]. Initially adsorption increases with increase in temperature by increase in the quantity of gas absorbed but at maximum temperature adsorption decreases. Chemisorptions on oxide or on metal surface involve considerable activation energies. Clean metal surface have comparable small but significant activation energy.

2.3.3 Surface morphology change with following parameters

- **Current density:** The surface roughness of plated films is changed with current density. Certainly the surface roughness is high at low current density and lowers with increase in current density. Therefore metal ions and electrons with high density generated at high

current densities will be redistributed over the surface according to the magnitude of their repulsive force. This cations redistribution over the substrate surface allows uniform distribution of the discharge sites, making the surface of plated films smoother [49]. Moreover the particle incorporation is also affected by current density [51-56] and hence influencing the properties of coating on the substrate.

- **Type of anions:** The surface morphology is affected by the molecular weight and size of anions, which are related to the solution viscosity and the diffusivity of anions toward the anode [49-50]. The resulting coatings will exhibit different mechanical, conductive, or electrochemical properties depending on the incorporated anion.

- **Temperature:** High solution temperature generally produces higher surface irregularities. The increasing solution temperature is closely related to the supply rate of metal ions, the diffusion distance of cations, and the surface diffusion distance of atoms and it can be easily seen that the increased diffusivity allows atoms to migrate a long distance over the substrate surface which producing large grains [34,49].

- **Surface agitation:** Agitation was performed by varying the speed of the magnetic stirring. With the increase in stirring speed, the film surface become more rougher and secondary surface irregularities were developed on the side face of the primary irregularities, as agitation of the solution supplies metal ions to the side face and thus made metal ion discharge possible at such sites. The agitation of the plating bath increased both microhardness and surface smoothness and decreased the residual stresses. Moreover it allows uniform distribution of particles in the suspension and prevents the settling of the dispersed particles at bottom [49].

- **Formation of dendrites:** Dendrites in plated films are often generated under conditions of low metal concentration/high current densities or of low current densities. An individual dendrite is generally a single crystal, but in some cases, it may be an assembly of fine grains. The films always begin as a uniform layer followed by dendrite formation on top of this layer.

This is consistent with the fact that metal ions present in close contact with the cathode are initially distributed uniformly over the substrate surface. After the layer formation, a metal-ion denuded zone is created over the surface of different thickness. Dendrites will then nucleate at such regions and their growth will be further accelerated through the tips, if current density becomes very high [49].

2.4 Pulsed Electrodeposition:

The traditional method of Electrodeposition is Direct Current (DC) electroplating. The modification of this method is done by the use of current interruption or even current reversal termed as pulsed electro deposition where not only the current or potential can be varied [44]. However, it is possible to vary parameters independently, pulse frequency, the current density and the duty cycle which is the ratio of pulse on time to the sum of on time and off time. The improved properties can be obtain as it is possible to get non dendritic, coherent deposits at much higher current densities than with the straight direct currents [44-45]. The additional higher over potentials results in higher nucleation rates which results in finer grain size. When the current is off during pulse plating, because of foreign substances may be either adsorbed or not the mechanical properties, the structure and texture can be different from those observed with conventional deposition [46-47]. The conditions of current density at the cathode, the electrolyte bath are bath composition, temperature and transport behavior and those of substrate (cathode) are crystallography and surface topography. A major limitation of the electrodeposits produced by direct current is rough deposits and porosity [48]. Pulse plating improves the deposit properties viz. hardness porosity, ductility, electrical conductivity, finer grain size plating thickness distribution. Numerous NC metals and alloys including Ni, Co, Cu, Zn and Ni-Fe [44-45] have been formed by pulse electrodeposition and reported to have unique properties.

2.4.1 Type of pulse waveforms:

Waveforms can be divided into two groups 1) **Unipolar**- The pulses are in one direction and pulses don't have polarity. 2) **Bipolar**- both anodic and cathodic pulses are mixed in bipolar pulses. There can be three major waveforms in pulse deposition

- Rectangular pulses**
- Periodic Reverse pulses**
- Symmetric Sinusoidal pulses**

Rectangular pulse deposition contains pulses of rectangular shapes and current and potential which are separated by zero current or potential.

Periodic reverse deposition The applied current or potential is sifted periodically from anodic and cathodic polarization.

Superimposed sinusoidal deposition The waveform is the sum of direct cathodic current (dc) and sinusoidal alternating wave current. Waveform may consist of both anodic and cathodic portion if dc offset is less than the amplitude of the sine wave.

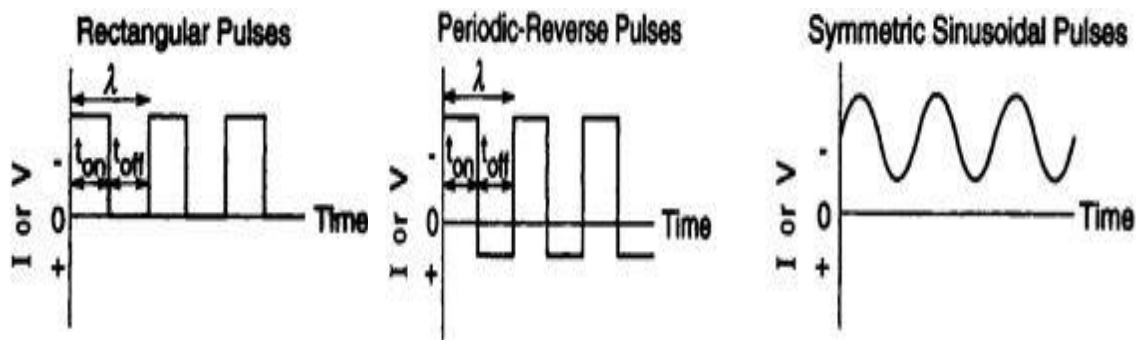


Figure 2.4: Major pulse waveforms for deposition.

2.4.2 Advantages of Pulse Electrodeposition (PED) over DC

- In electroplating, as the process continues a negative diffusion layer is formed around the cathode. When DC is used, this layer grows to definite thickness and obstructs the motion of ions from reaching the part. While with the pulse DC, current/potential is switched off during T_{OFF} and this layer gets discharged to some extent. Hence in PED this thin layer provides easier passage to the ions through the layer onto the part.
- In DC, the regions with high current density get depleted more of the ions than low current density regions hence, DC ions move to the cathode from higher concentration region to lower concentration region which results in depletion of ions. During T_{OFF} in PED, ions migrate towards the depleted region and during the T_{ON} more uniform distribution of ions is present for deposition. [57]

2.4.3 Advantages of pulse Electrodeposition (PED) technique

- PED significantly raises the limiting current density (IL) by replenishing metal ions in the diffusion layer during T_{OFF} .
- In PED, by modification of pulse parameters, deposits with desired composition, structure, porosity and hydrogen content can be obtained.
- Pulse plating enables the reduction of the additive requirement by 50–60%.

- Pulse DC eliminates thickness build up at high current density areas during current reversal and improves step coverage without pores reaching down to the substrate.
- In PED, homogeneity in deposition is increased due to high throwing power even at complex shaped parts.
- In PED layer density increases and elimination of pores occur.
- Resulting layer properties are improved example hardness.
- In enhances the acceleration of galvanic processes.
- In dispersion coating it enhances functionalizing by combination.

2.4.4 Significant outcomes of PED

- The deposited crystallite size which ranges in microns with DC reduces to nano range using pulse plating.
- Significant increase in density as well as homogeneity of the deposited metal layers is observed.
- The layer properties are improved.
- Alloy composition can also be controlled by altering the pulse sequence.
- Microstructure of the deposition can be tailored by modifying the pulse sequence.
- Systems like nickel, chromium, zinc, copper, gold, silver, rhodium and tin can easily deposited using pulse plating.
- Some processes like continuous strip plating and rack plating, barrel plating processes can be realized in practical.

2.4.5 Disadvantages of PED

There are very few and minor disadvantages associated with electrodeposition carried out using pulse DC, major disadvantages are:

- Generally the cost of a pulse rectifier is much higher than a DC unit. It involves a highly regulated and sophisticated design that costs more to manufacture.
- This technology requires skill person to think and plan ahead because a series of procedures needs to be followed in order to get the best results.

2.4.6 Technological Applications

Pulse plating is used on a larger scale for plating on electronic connectors and switch contacts. Development of less stressed pulse plated deposits made it easy to stamp and form contacts after plating. The economic gains achieved by using pulse DC surpass the relatively high cost of pulse power supplies. Manufacturers of semiconductor lead (Pb) frames prefer use of PC in order to increase the reliability of wire bonds and hence enhance the deposition rate. High-speed silver and gold-plating solutions are specially formulated for pulse deposition and are now available commercially. In Printed Circuit Boards (PCB) industry, there is a need for miniaturization of high-density interconnections which is possible by PED. For high-density circuitry applications in microelectronics industry, circuit traces can be brought closer together without shorting one another with the use of pulse technology. Pulse current can produce invariably fine-grained structures so that mechanical and physical, chemical properties of many metals and alloys can be enhanced. Pulse and the related techniques enable the production of newer types of deposits, which were considered impossible till now. Pulse technique may lead to some other electrochemical processes also in future (e.g., electro-discharge machining, electro-etching and electro-cleaning).

2.5 Electrophoreticdeposition (EPD):

Electrophoretic deposition is a process in which ceramic particles are suspended in a liquid medium, on the conductive substrate of opposite charge by the application of DC Electricfield. Compared to other advanced shaping techniques, the EPD process is versatile since it can be modified easily for a specific application. It offers important advantages in the deposition of complex compounds and ceramic laminates For example; deposition can be made on cylindrical, flat or any other shaped substrate with only minor change in electrode design and positioning. Also have advantages of short time, little restriction of the shape of substrates, needs simple apparatus [48, 57-58]. The basic difference between an electrophoretic deposition process (EPD) and an electrolytic deposition process (ELD) is that

the former is based on the suspension of particles in a solvent whereas the later is based on solution of salts, i.e., ionic species [60]. The (EPD) technique has a wide range of novel applications in the processing of advanced ceramic materials and coatings, such as in the fabrication of anti-oxidant ceramic coatings and wear resistant, fabrication of functional films for solid oxide fuel cells and advanced microelectronic devices as well as in the development of bioactive coatings for medical implants or novel composites, has increased the interest for its application in nanoscale assembly for advanced functional materials. And also has been used successfully for thick film of hydroxyapatite coating on metal substrate for biomedical applications, silica, nanosize zeolite membrane, luminescent materials, high-Tc superconducting films, gas diffusion electrodes and sensors, multi-layer composites, glass and ceramic matrix composites by infiltration of ceramic particles onto fibre fabrics, oxide nanorods, carbon nanotube film, functionally graded ceramics, layered ceramics, piezoelectric materials [51-66] etc.

2.5.1 Mechanism of electrophoretic deposition

If the charged colloidal particle suspended in an electrolyte solution, there is inhomogeneous distributions of ions, the concentration of ions are highest near solid surface and decreases from going outward from the surface. This inhomogeneity leads to the formation of double layer structure, which consists of Gouy layer (diffuse double layer) and stern layer as shown in the figure 2.5. The plane which separates these two layers is called Helmholtz plane. The electrically doubled layer plays vital role in interfacial electrical phenomena on the particle surface and particle-particle interaction in the electrolysis solution [49, 59, 67].

The bath ions distribution is mainly controlled by:

- Entropic force or dispersion
- Brownian motion
- Coulombic or electrostatic force

It is impossible to measure surface potential on the colloidal particles. We can measure potential near particle surface by calculating zeta potential.

2.5.2 Factors influencing EPD

The process being involved the deposition of charged particles from the suspension onto the conducting substrate (cathode) by the application of electric field. Thus two groups of parameters determines the characteristics of this process

- Parameters those related to the suspension such as Particle size, Dielectric constant of the liquid, conductivity, stability & viscosity of the suspension and Zeta potential.
- Parameters those related to the process including the physical parameters such as the electrical nature of the electrodes, the electrical conditions (voltage/intensity relationship, deposition time, etc.), effect of deposition time, applied voltage, concentration of the solid in the suspension.

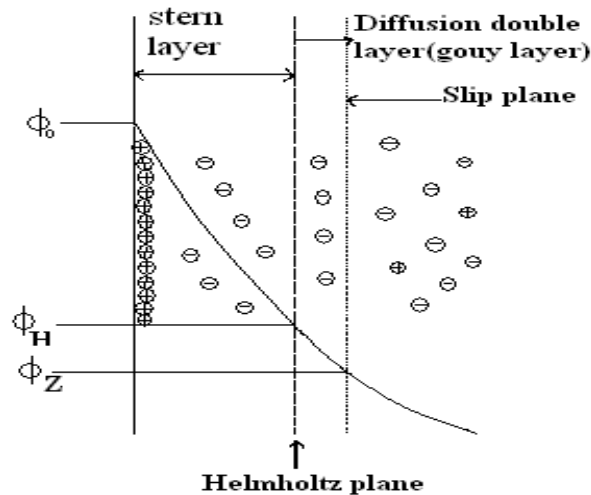


Figure 2.5: Schematic diagram of electrical double layer structure and the electric potential near solid surface with stern and Gouy layers (surface charge is assumed to be positive) [84].

2.5.3 Measurement of zeta potential of particles

Zeta potential is the potential difference between the dispersion medium and the stationary layer of fluid attached to the dispersed particle. It is the key factor in the electrophoretic and electrocodeposition processes. It is a very good index of the magnitude of the electrostatic repulsive interaction between particles. It gives the degree of stability of the suspension.

Zeta potential is widely used for quantification of the magnitude of the electrical charge at the double layer. Zeta potential is often the only available path for characterization of double-layer properties.

Zeta potential can also point out the measure of repulsion between similarly charged particles in dispersion. Solution having small particles directs the high zeta potential, i.e. the solution or dispersion will resist aggregation. At low potential, attraction exceeds repulsion and the particles get flocculated. Hence colloids with high zeta potential (negative or positive) are electrically stabilized while colloids with low zeta potentials tend to coagulate or flocculate [49, 60, 67]. The most important factor that affects zeta potential is pH of the suspension. Let

us suppose that a particle in suspension with a negative zeta potential. If further alkali is added to this suspension then the particles will likely acquire a more negative charge which indicates lower pH value. If acid is then added to this suspension a point will be reached where the negative charge is neutralized. Any further addition of acid can cause a buildup of positive charge, indicates the increase in the pH.

In general, a zeta potential versus pH curve will be positive at low pH and lower or negative at high pH. There may possibly is point where the curve passes through zero zeta - potential. This point is called the isoelectric point and is very important from a practical consideration. It is the point where the colloidal system is at least stable.

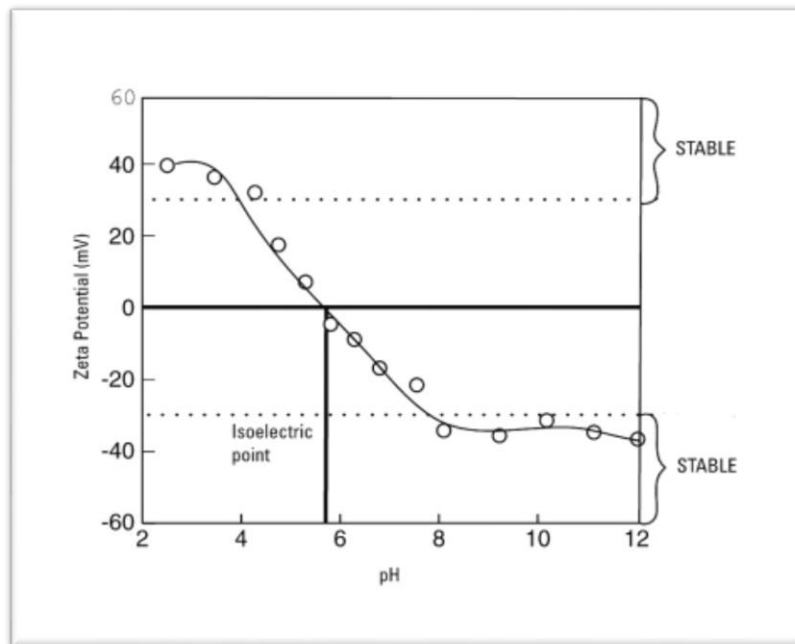


Figure 2.6: pH Vs Zeta potential [83].

In the Figure 2.6 it can be seen that if the pH of dispersion is above 8 or below 4 there is sufficient charge to confer stability. Conversely if the pH of the system is between 4 and 8 the dispersion is likely to be unstable. This is most likely to be the case at around pH 6 (the isoelectric point). Electrophoretic deposition is the process of depositing charged powder particles dispersed or suspended in the liquid medium.

2.6 Electrocodeposition

It is the process of particle incorporation during the electrolytic deposition of metal, which involves both the processes, electrodeposition of metal from electrolyte solution and electrophoretic deposition of the small sized particles from the suspension, the schematic of the process is as shown in below Figure 2.7. This process produces composite films

consisting of a metallic matrix containing a dispersion of small particles. The particles of pure metals, ceramics, and organic materials, for example oxide or carbide particles, such as Al_2O_3 , SiC , TiO_2 , WC , SiO_2 or diamond, a solid lubricant, such as PTFE, graphite or MoS_2 , or even liquid-containing microcapsules ranging in size from sub-micron to 100 μm in diameter are used as dispersed second phase particles, and embedded in electroplated Cu, Ni, Co, Cr, and various alloys [8-13, 68].

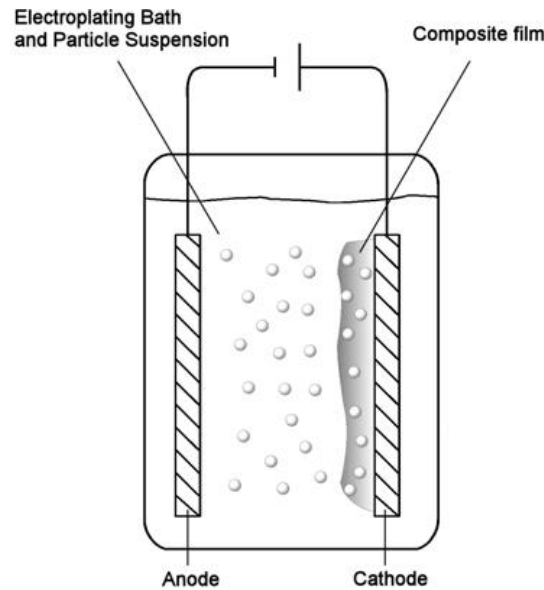


Figure 2.7: Schematic of Electrocodeposition process

The advantages of electrocodeposition technique over other coating methods are the uniformity of deposition even for complex shapes, reduction of waste often encountered in dipping or spraying techniques, low levels of contamination, the ability to produce functionally-gradient material and to continuously process parts. In addition, this process avoids the problems associated with high temperature and high pressure processing.

The applications of these electrocodeposited coatings include wear and abrasion resistant surfaces, lubrication, high hardness tools, dispersion-strengthened alloys, and for protection against oxidation and hot corrosion [69-71]. And also Electrocodeposition has been used to produce high surface area cathodes which have been used as electro catalysts for hydrogen electrodes in industrial water electrolysis [68]. The first application of electrodeposited composite coating was the Ni/SiC coating used as the wear-resistant improvement in the Wankel engine by Metzger et al., in 1970 [72]. The metal matrix composites have been synthesized using Electrocodeposition include Ni-SiC and Ni-Co/ Al_2O_3 , Ni- TiO_2 , Ni-Co, Ni-Zn, Ni-Fe, Co-17 W, Co-P, Pd-Ni, Cu- TiO_2 , Cu- Al_2O_3 , Cu- ZrO_2 , Cu- ZrB_2 , Cu/CNTs, , Cu-WC, Ni-Fe-nano- Si_3N_4 , Co-Ni-nano- Al_2O_3 , Zn-Ni-nano-SiC etc. [8-13, 68].

2.6.1 Mechanism of electrolytic co-deposition

As reported above that electrocodeposition mechanism based on two types of mechanism and they are electroplating and electrophoretic deposition mechanisms [49, 59]. By using electroplating method, chromium is deposited on the cathode surface where as by electrophoretic method, the second phase particle deposited on the cathode surface. This coated surface is also called as composite coating. The positive charge metal ions and gained the positive electric charge (if pH is less than 7) is absorbed by the second phase colloid solution suspended in the electrolytic solution absorbs. The particles reach the cathode surface driven by the electrostatic attraction and electrolyte conventions. The retaining capacity of the particles on the cathode surface depends on bonding force between them and also it depends on the interfacial energies of cathode-electrolyte, particle-electrolyte.

2.6.2 Effect of electroplating process parameters on co-deposition

(a) Bath composition

The composition of the codeposition bath is not only defined by the concentration and type of electrolyte used for depositing the matrix metal, but also by the particle loading in suspension, the pH, the temperature, and the additives used.

(b) Particle Loading in Suspension

Particle loading or concentration of particles in the suspension is important factor which affects the amount of particle concentration in the deposits. At low loadings, codeposition is limited by the supply of particles to the electrode surfaces (cathode) leads to small amount of particles in the deposition. As the particle loading increases, supply of particles to the electrode increase so does the incorporation level in the deposition increases. But at the highest loadings (beyond which particle settling becomes significant), the increase in incorporation is not proportional to the increase in loading. For the parallel plate system, the amount of incorporation has been found to increase with increasing particle loading following a Langmuir-adsorption type isotherm [72].

(c) Bath Agitation

Increase in the bath agitation in the parallel plate electrode setup has been found to increase the amount of particles codeposited within the electroplated film for the Ni-Al₂O₃ and Ni-TiO₂ systems [74]. When the agitation is increases, a greater number of particles arrive at the electrode surface and the amount of particle incorporation in the metal film increases. However, if the agitation is too intense, the residence time for the particles at the electrode surface is insufficient and the particles are swept away before they can be incorporated into

the growing metal film. Also, the amount of codeposition has also been observed to decrease in the Cu-SiC and Cu-CrB₂ systems with increasing agitation [75].

(d) Surfactant

The codeposition of particles increases with increasing the concentration of surfactant in the solution, this is due to the modification of the surface charge of the particles in the suspension by the absorbed molecules or ions, thereby decreasing agglomeration of particles and promoting the electrophoretic migration of the suspended particles. Thus increases in the amount of particle concentration in the film with homogenous distribution.

(e) Current Density

Current density plays an important role in controlling the deposition rate which will in turn affect the concentration of incorporated particles in the coatings. It also influences the thickness of the composite films, such that as the current density increases the thickness of the coatings increases. When the current density is increased, the amount of particle incorporation obtained has been found to increase for the Ni-TiO₂ system with a relatively slow agitation [75], decrease for natural or synthetic diamond in Ni [76] and for Cr particles codeposited in Ni [77] and to be unaffected when codepositing alumina in Ni. It also plays a role in the thickness of the deposited films.

(f) Particle Characteristics

Particles can be characterized by their composition and crystallographic phase, as well as by their size, density, and shape. The particle composition can have a dramatic impact on the amount of incorporation obtained for a particular bath composition. For instance three times more TiO₂ than Al₂O₃ has reportedly [73] been incorporated into a Ni matrix, under the same deposition conditions. The particle size also effects on the amount of codeposited particles in the composite coatings. For example when the particle size in the electrolyte increases then amount of adsorbed ions on the surface increases, which leads to the increase in the migration velocity of the particles and also results in a higher columbic force of attraction, leads to increase in the amount of the particles. But the density of particles in the coating decreases as the particle size in the electrolyte increases. For example increasing the particle size resulted in an increase in the amount of incorporation for Ni-Al₂O₃, Ni-SiC, Ni-Cr, Cu-P, and Cu-Al₂O₃ [68]. However, other researchers found particle size to have a negligible influence on the amount of incorporation for Ni-Al₂O₃ and SnNi-SiC [68].

2.7 Brief Review on Cr composites coating

SL NO	AUTHOR	YEAR OF PUBLICATION	MATERIAL USED	OBJECTIVE OF PAPER	RESULT OBTAINED
1	Sun Ke-Ning et al	1996	Cr-Al ₂ O ₃ composite coatings	To study the effect of various plating variables on the Al ₂ O ₃ content.	0.7-1.0 wt% of Al ₂ O ₃ increases the hardness upto 1300 HV and wear resistance increases by two to six times as compared to Cr coating.
2	Jifeng Gao et al	2011	Cr-Al ₂ O ₃ /SiC composite coatings	To increase the SiC content in Cr-based coatings.	The Al ₂ O ₃ /SiC particles significantly enhanced the corrosion resistance of the composite coating in 0.05 M HCl solution.
3	M.RezaeiSameti et al	2012	Cr-WC composite coatings	To study the effect of pulse electroplating parameters such as current density and duty cycle on the amount of incorporated WC particles and morphology of the coatings	with the decrease in duty cycle, the volume percentage, hardness and wear resistance of coating increased and by increasing the current density up to 15 A/dm ² , the both of Volume percentage and hardness will increase. Finally the optimum wear resistance was achieved at the current density of 8 A/dm ² , duty cycle of 50%.
4	S. Surviliene et al	2008	Cr- ZrO ₂ composite coatings	To study the effect of ZrO ₂ particles on corrosion behaviour of Cr coating	samples plated in bath containing ZrO ₂ exhibited improved protective properties as a result of the structural characteristics of the coatings obtained; namely, the size and shape of pores

2.8 wear

It is a process of removal of material from solid surfaces either one or both of two in solid state contact, when two solid surfaces are in sliding or rolling motion together [76]. The rate of removal is generally slow, but steady and continuous. The five main categories of wear and the specific wear mechanisms that occur in each category are shown in figure 2.8.

2.8.1 Abrasive Wear

Abrasive wear occurs when material is removed from one surface by another harder material, leaving hard particles of debris between the two surfaces. It can also be called scratching, gouging or scoring depending on the severity of wear. Abrasive wear can be classified under two conditions:

1. Two body abrasion; in this state one surface is harder than the other rubbing surface as shown in figure. Examples in cutting, mechanical operations are grinding and machining.
2. Three body abrasion; in this condition a third body, generally abrasive or a small particle of grit lodges between the two softer rubbing surfaces, abrades one or both of these surfaces, as shown in figure 2.9.

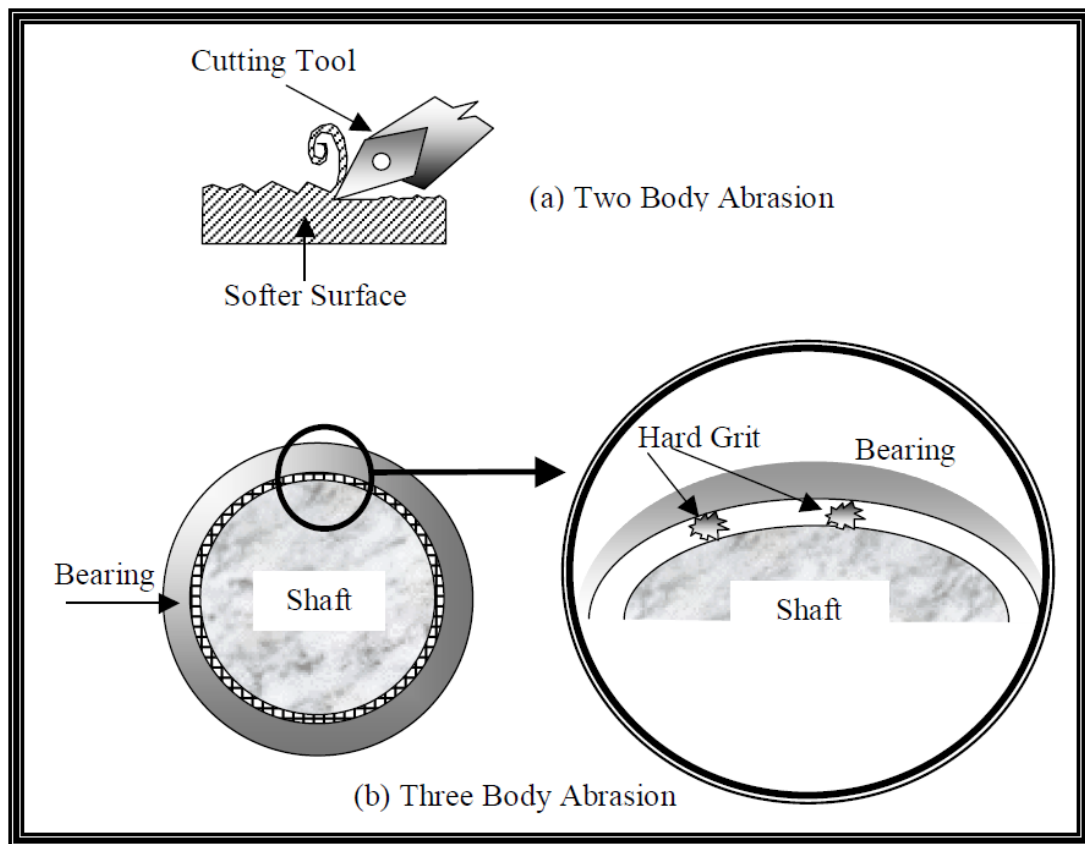


Figure 2.8: Flow chart of various wear mechanisms [76].

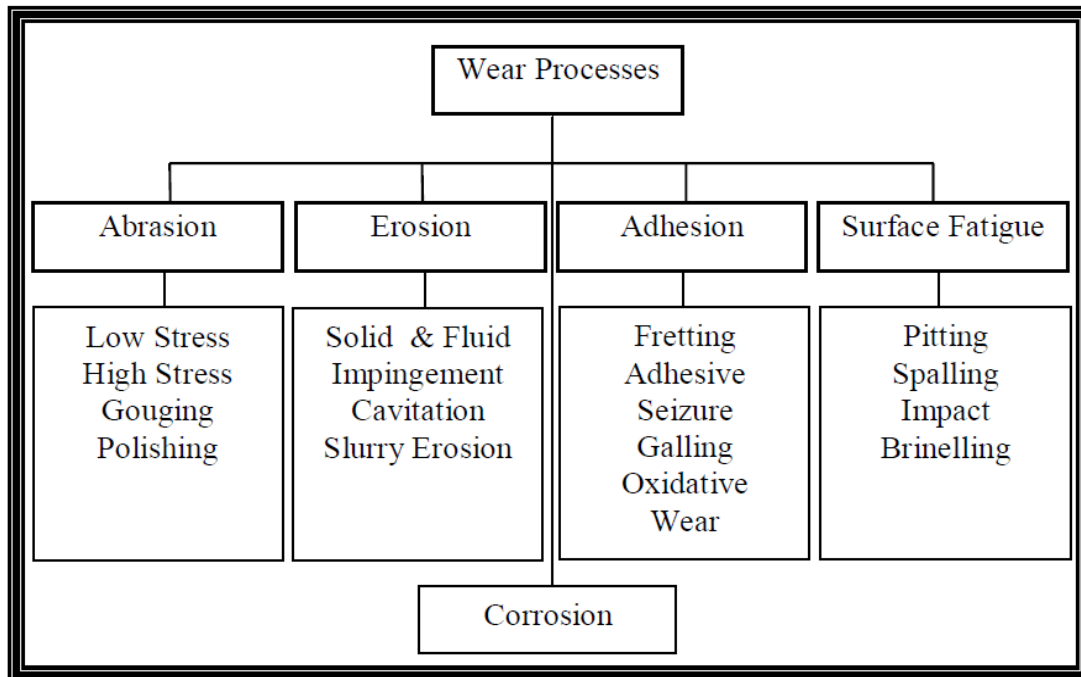


Figure 2.9: Schematic of abrasive wear phenomena [76].

In the microscale, the abrasive wear process is where in the softer surface the asperities of the harder surface force down into, with plastic flow of the softer surface occurring around the harder asperities, as shown in figure. When a tangential motion is imposed this often leads to microcutting, microploughing, and microcracking. Abrasive wear may be reduced by the introducing of hydrodynamic or elastohydrodynamic lubricants at various film thicknesses to separate the surfaces and to wash out any contaminant particles. Research shows that using the various thermally sprayed techniques including the HVOF process and correct coating material can greatly benefits resistance to abrasive wear [77].

2.8.2 Erosive Wear

The impingement of small drops of liquid or gas or solid particles often cause erosion of materials and components. Solid particle impact erosion has been receiving increasing attention especially in the aerospace industry [78]. Examples include the ingestion of sand and erosion of jet engines and of helicopter blades. As shown in figure2.11 the erosion mechanism is simple. Solid particle erosion is a result of the impact of A solid particle, with the B solid surface, resulting in part of the surface B been removed. The impinging particle may vary in form as well as in composition.

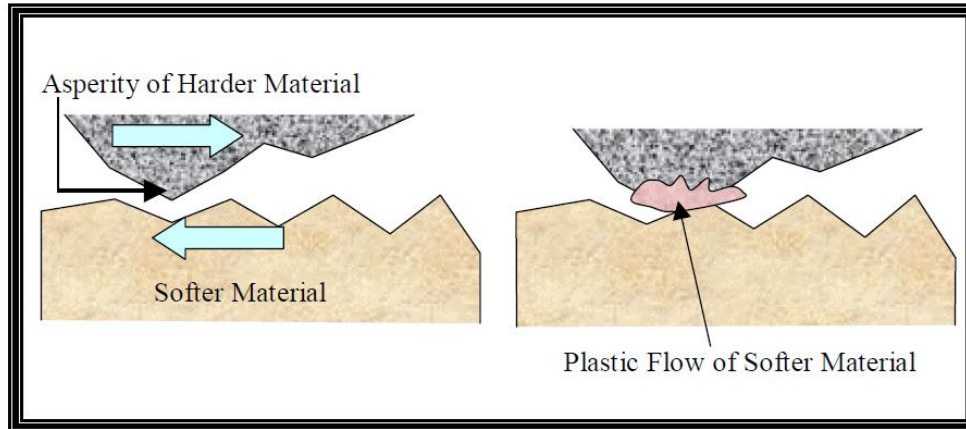


Figure 2.10: Abrasion in the microscale [76].

The response of engineering materials to the impingement of liquid drops or solid particles varies greatly depending on the materials properties; class of material and the environmental parameters associated with the erosion process, such as impact angle, impact velocity and particle size. Movement of the particle stream relative to the surface and angle of impingement both have a significant effect on the rate of material removal [79]. The erosive effects on materials at high temperatures are important for the selection of turbine engine materials in the aerospace industry.

Cavitation erosion occurs when a solid and a fluid are in relative motion, due to the fluid becoming unstable and bubbling up and imploding against the surface of the solid, as shown in figure 2.10. Cavitation damage generally occurs in such fluid-handling machines as marine gates, propellers, hydrofoils, dam slipways, and all other hydraulic turbines, according [76]. Cavitation erosion roughens a surface much like an etchant would.

2.8.3 Adhesive Wear

Adhesive wear is often called galling or scuffing, where interfacial adhesive junctions lock together as two surfaces slide across each other under pressure [76]. As normal pressure is applied, local pressure at the asperities become extremely high. The yield stress is exceeded very often, and the asperities deform plastically until the real area of contact has increased sufficiently to support the applied load, as shown in figure. Without lubricants, asperities cold-weld together and form new junctions. This wear mechanism not only destroys the sliding surfaces, but the generation of wear particles can cause cavitation and can lead to the failure of the component. The sufficient supply of lubricant resolves the adhesive wear problem occurring between two sliding surfaces.

2.8.4 Surface Fatigue

When mechanical machinery move in periodical motion, stresses to the metal surfaces occur, often leading to the fatigue of a material. All repeating stresses in a rolling or sliding contact can give rise to fatigue failure. These effects are mainly based on the action of stresses on the surfaces, without the need of direct contact of the surfaces under consideration.

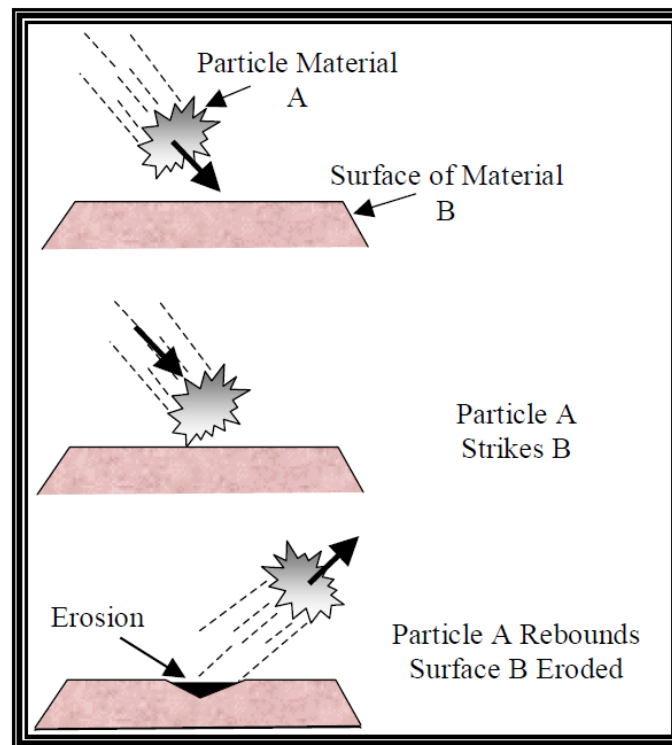


Figure 2.11: Schematic of erosive wear [76].

When two surfaces slide across on one other, the maximum shear stress lies some distance below the surface, causing microcracks, which lead to failure. These cracks initiate at the point with the maximum shear stress, and propagate to the surface as shown in figure 2.12. Materials are not often perfect; hence the exact position of ultimate failure is influenced by inclusions, microcracks porosity, and other factors. Fatigue failure requires number of stress cycles and often predominates after a component has been in service for a long period of time.

2.8.5 Corrosive Wear

In corrosive wear, the dynamic interaction between mating material and the environment surfaces play a significant role, whereas the wear due to adhesion, abrasion and fatigue can be explained in terms of stress interactions and deformation properties of the mating surfaces.

In corrosive wear first the linking surfaces react with the environment and reaction products are formed on the surface asperities. Attrition of the reaction products then occurs as a result of crack formation, and/or abrasion, in the contact interactions of the materials.

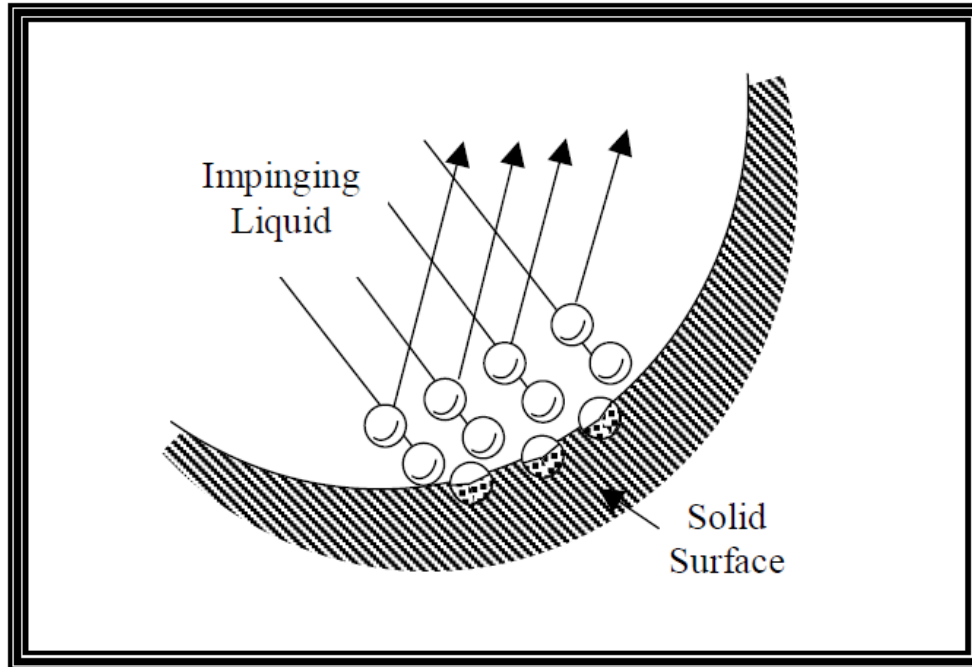


Figure 2.12: Schematic of fatigue wear, due to the formation of surface and subsurface cracks [76].

This process results in increase in reactivity of the asperities due to changes in the asperity mechanical properties and increased temperature. Thermally sprayed coatings applied to various material surfaces, such as those depositing using the HVOF process, have proved an effective tool in the prevention of corrosion.

CHAPTER 3

EXPERIMENTAL

Sample Preparation

Plating bath Solution Preparation

Particle Size Analysis

X-Ray Diffraction Studies

Microstructural Studies

Surface Mechanical Property Study

CHAPTER 3

EXPERIMENTAL

3.1 Sample preparation

The specimens with approximate dimensions of 12 mm x 12 mm x 4 mm were cut from hot rolled SAE 1020 grade mild steel bar with nominal composition of % C: 0.18-0.22; % Si: 0.1-0.35; % Mn: 0.6-0.7; % Al: 0.01(max); %S: 0.02(max); % P: 0.03 and balance Fe (in wt.%). This steel was selected for the present study as model plain carbon steel used for structural applications. Samples were prepared by grinding and polishing by using 250, 400, 600 and 800 grit polishing papers. In this way the mirror polished substrates were prepared for deposition. Holes were made on the samples to dip the samples in the electrolyte solution and to supply current by attaching copper wire to the hole.

3.2 Particle size analysis

The particle size of fine ZrO_2 powder which was procured from Inframat Advanced Materials, Formington, USA was checked by Malvern Zetasizer nano series Nano-ZS model instrument. Before measuring particle size, the particle was dispersed in the aqueous bath by 20 minute magnetic stirring followed by 10 minutes ultrasonication. Figure shows the photograph of Malvern Zetasizer which can measure particle size from nanometer size to micron size, and zeta potential of suspended particle in a solution. To verify the data available in literature, variation of zeta potential against pH was estimated by the same instrument so that stable suspension pH can be obtained and pH for required cathodic deposition of the ceramic particle can be estimated.

3.3 Plating Solution Preparation

For electro co-deposition of Cr/Cr- ZrO_2 , standard solution was used as the basic plating bath of Cr coating. The parallel plate electrode configuration and bath without addition of surfactant and additives, is used for the codeposition ZrO_2 of in the chromium matrix. The bath compositions and parameters used for Cr coatings are reported in the Table 3.1. As the isoelectric point of ZrO_2 was determined around 5.35, so the pH of the solution maintained below this value (pH 1.14) so that the particles in the suspension acquire positive charge in the acid solution and deposited into the growing metal on cathode. A stainless steel plate was used as anode where as the prepared specimens were used as cathode. Before deposition the solution was allowed for magnetic stirring for 30minutes for homogenous dispersion of the ZrO_2 powder in the solution.



Figure 3.1: Nano zeta sizer (Model: Nano ZS, Malvern instrument).

Magnetic stirring was also allowed for stirring of the bath during entire deposition so that the sedimentation of powder particles in the solution is prevented and they can be homogeneously dispersed during deposition in the chromium matrix. The temperature was maintained by the use of a hot plate and the electro-deposition was controlled by a DC source (APLAB 7103). Out of 10 mild steel samples, one was to be used as a reference sample; electrodeposited by dc and for other samples the deposition was done by pulse dc by varying frequency (viz. 4 kHz, 8 kHz, 12 kHz) and duty cycle (viz. 10, 30 and 50). After deposition the samples were washed with distilled water, kept in the paper and preserved for Characterizations.

Table 3.1: Overview of Bath composition and Plating condition

Electrolytes	Chromic acid (Cr_2O_3)= 250 g/l
	Sulphuric acid (H_2SO_4)= 2.5 g/l
	Zirconia (ZrO_2) :15
Operating Conditions	Temperature: $47 \pm 2^\circ \text{C}$
	Cathode current density: 7 mA/mm^2
	Anode: Stainless steel
	cathode :Mild steel
	Electrolyte volume : 250 ml
	pH:1.14
	pulse frequency :Without pulse, 4 kHz, 8 kHz, 12 kHz
	pulse Duty cycle: Without pulse, 10, 30, 50

3.4 X-ray diffraction studies

X- Ray Diffraction studies of all the deposited samples were performed by using, Philips X'Pert system with Cu K α radiation ($\lambda= 1.5418 \text{ \AA}$) to judge the phases formed, to calculate the crystallite sizes and also to determine the Texture Coefficient (TC) of the deposits. The same was also done for pure chromium sample which was used as substrate and for raw powders of ZrO₂. The XRD was carried out with 2θ range of 20°-100° with scan rate of 3°/min.



Figure 3.2: Philips X'Pert system

3.5 Microstructural studies

3.5.1 Scanning Electron Microscope (SEM) studies

Scanning Electron Microscopic studies were performed to view the morphology of the coatings, distribution of the particles, to determine the composition of the coatings by using JEOL 6480 LV scanning electron microscope (SEM) equipped with an energy dispersive X-ray (EDX) detector of Oxford data reference system which is shown in the below Figure 3.2.



Figure 3.3: JEOL 6480 LV scanning electron microscope (SEM)

3.6 Surface mechanical property studies

3.6.1 Microhardness Measurement

Microhardness of the composite coatings (Cr-ZrO_2) and pure chromium coatings were determined by using LECO LM700 microhardness tester which is shown in Figure 3.3. The machine have minimum 1gf and maximum 1000 gf load, Dwell time 5-99sec and Knoop or Vickers indenter is included . The test was carried out with 50 gf load for 5 seconds to ensure that the indentation is up to the coating surface only. The hardness values were taken at 5 different places on the surfaces and average of these values were considered in the results.



Figure 3.4: LECO LM700 Microhardness tester

3.6.2 Wear Behaviour of the Coatings

The sliding wear resistance of the composite coatings and pure chromium coatings were evaluated by using ball on plate type wear testing instrument having a diamond ball (SAE

52100) indenter of 4 mm diameter. DUCOM TR-208-M1 ball on plate wear tester was used for this study to evaluate the wear resistance of all the coated samples with 20N load, 10rpm speed and 15minutes duration time. Graphs were plotted against Sliding distance vs. wear depth to compare the wear resistances of the different samples. Scanning Electron Microscope (SEM) was used to analyze the surface damages caused by the wear testing machine to get an idea about the wear mechanism.

CHAPTER 4

RESULTS AND DISCUSSIONS OF PURE CHROMIUM COATING

XRD analysis

Microstructural characterization

Surface Mechanical properties

RESULTS AND DISCUSSIONS OF PURE CHROMIUM COATING

4.1 XRD analysis

Figure 4.1 shows XRD patterns of different coatings as mentioned in the caption. Figure 4.1 (a) demonstrates that with 4 kHz frequency, the (200) texture increases with increase in duty cycle values. Similar peak intensities were also observed with no pulse condition. In case of higher frequency the current rise up and die down delay became almost negligible and so, higher frequency is sensed by the sample as almost continuously flow of current. Thus texturing nature is similar in no pulse sample and high frequency PED samples.

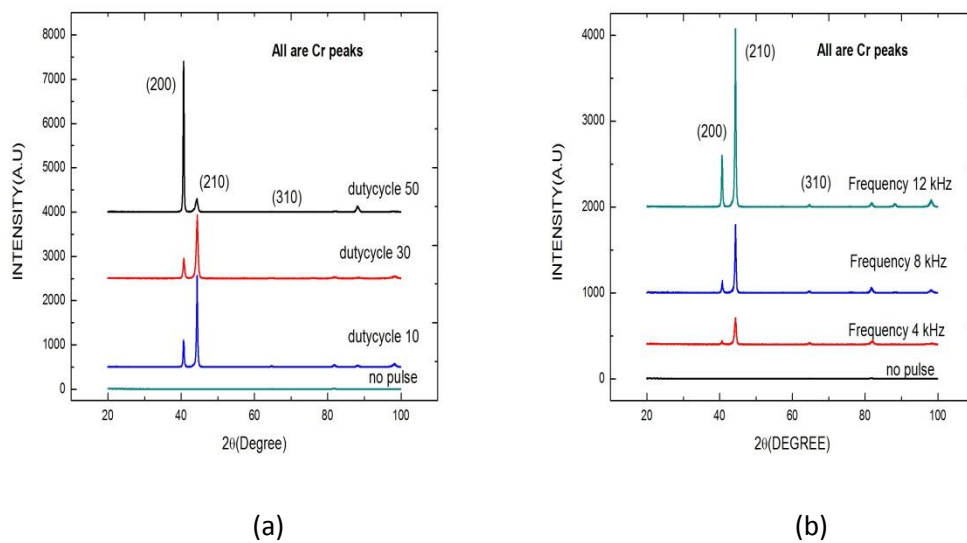


Figure 4.1.(a) XRD pattern of Cr coating at different Duty cycle(10,30,50)% at 4 kHz frequency(b) XRD pattern of Cr coating at different frequencies(4,8,12) kHz at duty cycle 10.

From the XRD pattern of different relative peak intensities corresponding to different planes of chromium with change in deposition parameters was observed.

The crystallite sizes of all the coated samples were calculated by using Scherrer formula given by equation are given in below Table 4.1 & 4.2. The crystallite sizes observed were all are less than 100 nm. The Scherrer equation is given by [86-87].

$$D = \frac{0.94\lambda}{\beta \cos\theta}$$

Where D is the crystallite size, β is the full width at half maximum (FWHM) of the diffraction peak, λ is the wavelength of the incidental X-ray (1.54 \AA) and θ is the diffraction angle.

For systematic study of the texturing, texture coefficient (TC) of each plane for all the samples were calculated using the following equation [85].

$$TC(hkl) = \frac{I_{(hkl)}/I_{0(hkl)}}{\sum\{I_{(hkl)}/I_{0(hkl)}\}} \times 100\%$$

Where $I_{(hkl)}$ is the intensity obtained from textured sample and $I_{0(hkl)}$ is the intensity of the standard oriented sample i.e., from JCPDS data. Table 4.1 shows such TC data calculated on four different planes, i.e. (200), (210), (310).

The above Figure 4.1 and Table 4.1 show the comparable XRD patterns for. From the figure it is evident that all the peaks showing were belonging to the Cr.

Table 4.1 Effect of different frequencies on texture coefficient of Cr coating

Cr Coating/sample	Texture coefficient			Crystallite size (nm)
	(200)	(210)	(310)	
Without pulse	0.00	0.27	0.73	44
4-10	0.25	0.74	0.01	31
8-10	0.15	0.82	0.03	32
12-10	0.11	0.83	0.07	22

From the Table 4.1 & Figure 4.1 (b) it can be observed that (210) is the most intense diffraction line (texture) in Cr coatings at 12 kHz frequency. The quality of the (210) texture was obviously affected by the frequency. At both cases (i.e. 4 kHz and 8 kHz) the intensity of (210) is less (8%) and (1%) respectively which is accompanied by increase in the intensities of 200) and (310) lines. As the frequency increased from 4 kHz to 8, 12 kHz the intensity of (210) texture increased by 8% and decrease by 1% respectively, the increase was accompanied by decrease in the intensities of (200) lines, this is due to higher over potential which affects the nucleation and growth of crystallites.

From the Table 4.2 & Figure 4.1(a) it can be observed that (200) is the most intense diffraction line (texture) in Cr-ZrO₂ composite coatings at 50 % duty cycle. At both cases (i.e.10 % and 30 %) the intensity of (200) is less (69% and 66%) which is accompanied by increase in the intensities of (210) and (310) lines. In without pulse samples the most pronounced diffraction line is (310).

Table 4.2 Effect of different dutycycles on texture coefficient of Cr coating

Cr Coating/sample	Texture coefficient			Crystallite size (nm)
	(200)	(210)	(310)	
Without pulse	0.00	0.27	0.73	44
4-10	0.25	0.74	0.01	31
4-30	0.28	0.72	0.00	61
4-50	0.94	0.06	0.00	32

In the summary from the above discussions on texture study of Cr-ZrO₂ systems it can be concluded that the observed texture is due to the influence of frequency, duty cycle.

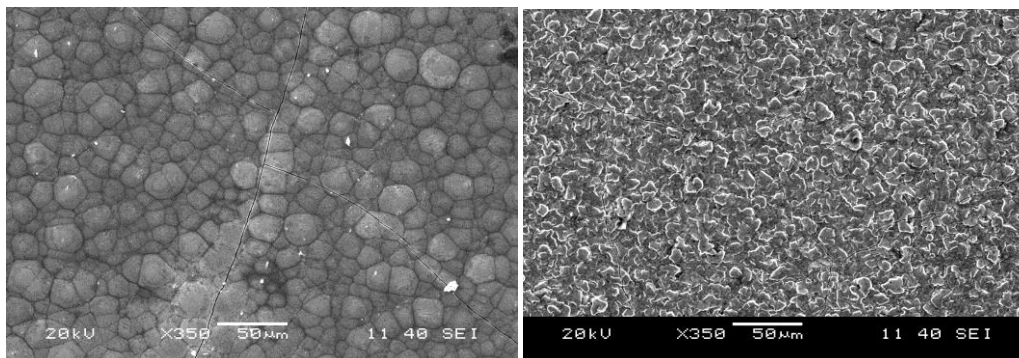
In Table 4.1 and 4.2 it can be observed that in general the crystallite size of Chromium coating is fine in nature as calculated from Scherrer equation.

4.2 Microstructural analysis:

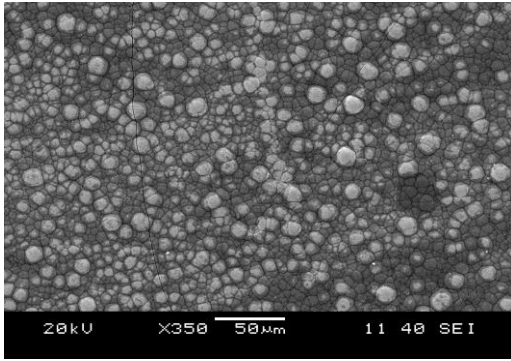
4.2.1 SEM and EDS analysis

After electrodeposition for 1 hour, the microstructure of the coating surface was investigated by SEM. Figure. 4.2 show such micrograph taken at 350X magnification for different coating conditions. All the samples at higher magnifications can be seen in figure 4.3 and 4.4.

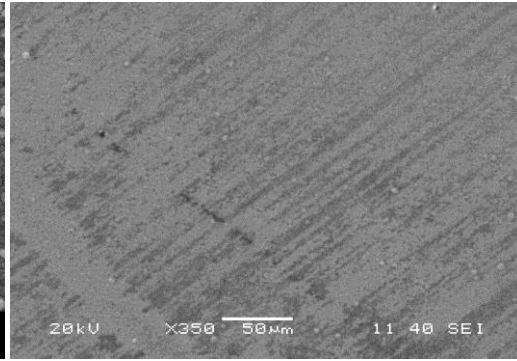
The surface morphology at no pulse shows globular shape nodule/grain with some microcracks whereas with increasing frequency the size is decreasing i.e. In pulsed electrodeposition (PED) samples finer asperities can be observed compared to no pulse sample. This may due to be high rate of nucleation leading to finer grain size. Microcracks are inherent properties of Cr coating reported by other reserachers also. But extent of the crack was low at higher frequency.



(a) Without pulse



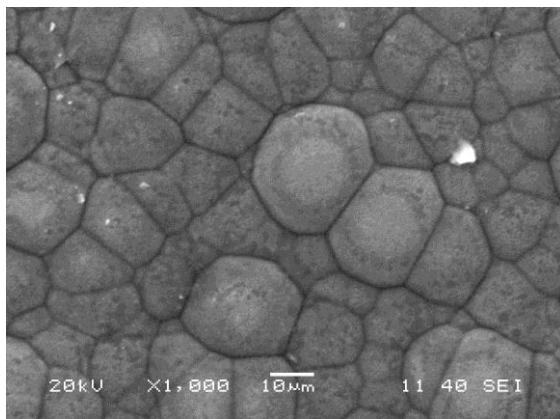
(b) Frequency 4kHz and duty cycle 50



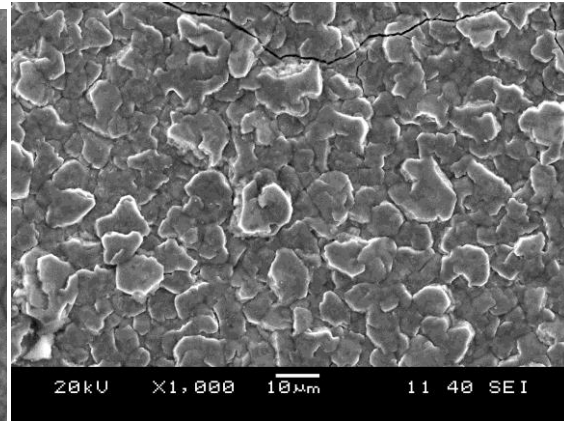
(a) Frequency 8kHz and duty cycle 50

(d) Frequency 12 kHz and duty cycle 50.

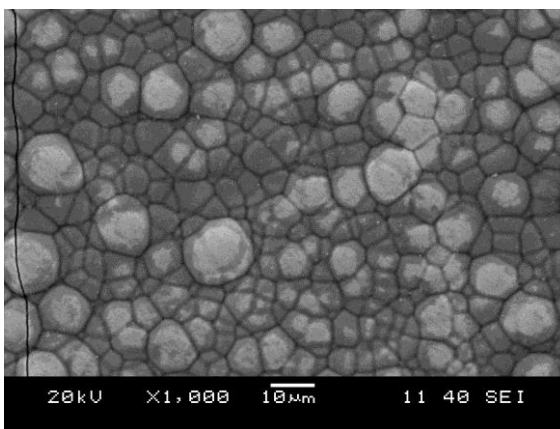
Figure 4.2 .SEM image of surface morphology of Cr coatings at different pulse parameters with 350x magnification



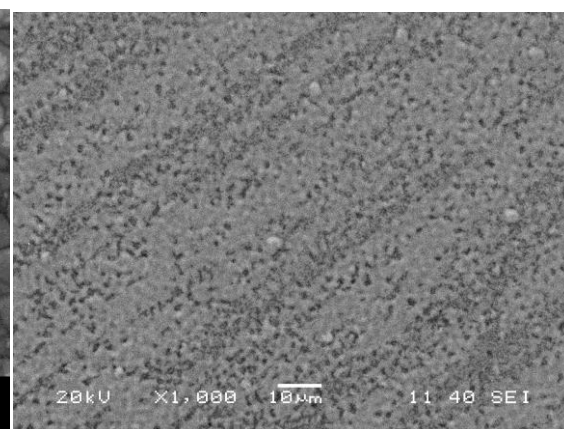
(a) Without pulse.



(b) Frequency 4 kHz and duty cycle 50.

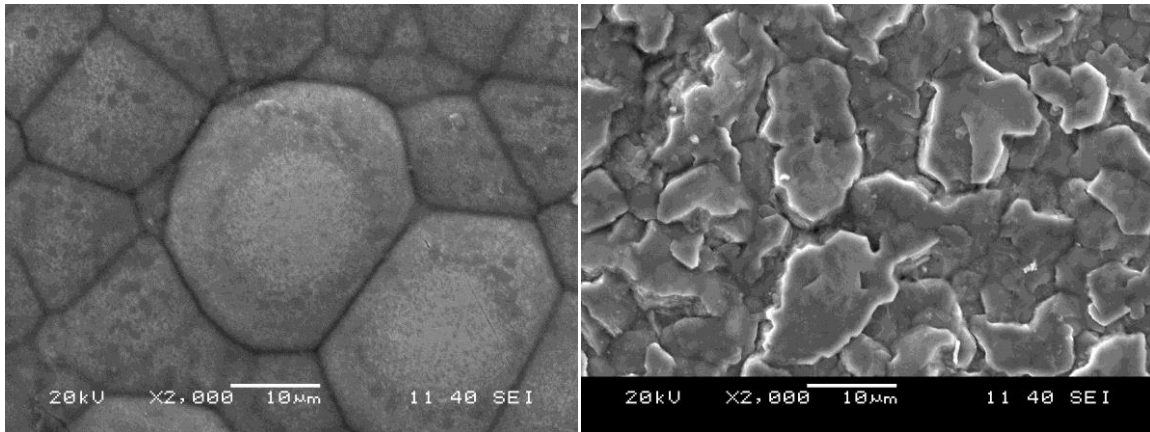


(c) Frequency 8 kHz and duty cycle 50.



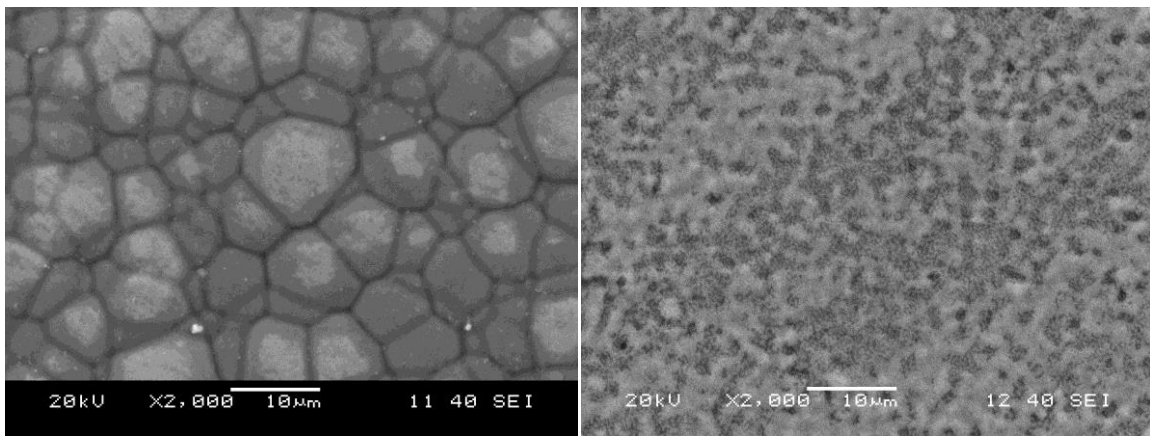
(d) Frequency 12 kHz and duty cycle 50.

Figure 4.3. SEM image of surface morphology of Cr coatings at different pulse parameters with 1000x magnification



(a) Without pulse.

(b) Frequency 4 kHz and duty cycle 50.



(c) Frequency 8kHz and duty cycle 50.

(d) Frequency 12 kHz and duty cycle 50.

Figure.4.4. SEM image of surface morphology of Cr coatings at different pulse parameters with 2000x magnification

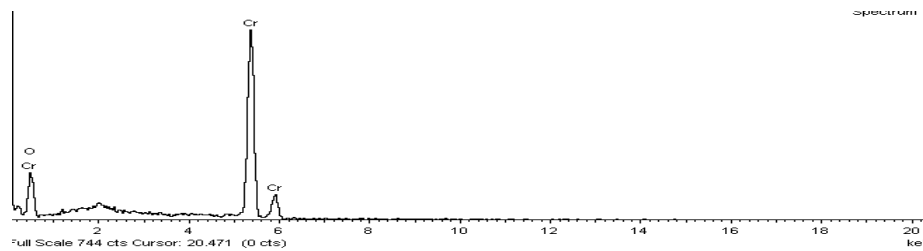


Figure.4.5. Sample EDS analysis of the Cr coating.

Figure 4.5. shows the EDS analysis of the as-deposited coating. It shows chromium only and similar EDS data were obtained in other parameters also.

4.3 Surface Mechanical properties:

4.3.1 Microhardness measurement

Figure.4.6. shows variation of microhardness vs. frequency on the coated surface as function of different dutycycle for each coating.

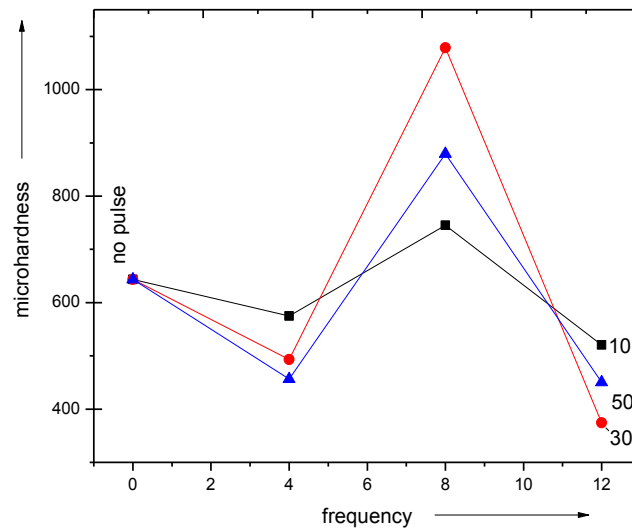


Figure 4.6. Variation of Microhardness with Frequency (i.e 4,8,12 kHz) at Dutycycle (i.e. 10, 30, 50).

The microhardness of the pure chromium coatings were measured by using Leco LM700 microhardness tester by applying 10gf load for 15 seconds in order to ensure that the microhardness values are not affected by the substrate. Figures 4.6 shows the effect of frequency and dutycycle on microhardness of Cr coating developed at frequency 4 kHz, 8 kHz, 12 kHz and dutycycle 10, 30, 50 without addition of any surfactant and additives to the bath. In the present work the hardness values were observed are mainly depending on preferred crystal orientation (Texture) of the matrix phase and marginal effect of grain size.

When the frequency increased from 4 kHz to 8 kHz, the hardness values increased and at 12 kHz a decrease in hardness values were obtained. In case of Cr coatings by PED technique at 4 kHz in all the cases 10, 30, 50 less hardness values were reported which is due to the random crystalline orientation (Table 4.1 & 4.2) which leads to decrease in the intensity of (210) texture, and increase in intensity of (200) plane this may be co related with [100] texture associated to deposits with minimum hardness and maximum ductility [88]. The

minimum hardness for (200) diffraction line is attributed to lower angle between (200) and (100) planes, which leads to lower strain energy, the strain energy increases as the angle increases [89-90]. The higher intensity of (310) plane leads to higher hardness this is due to its highest angle with the (100) planes. The higher intensity of (210) plane leads to higher hardness this is due to its less active slips [91]. Moreover the higher hardness values in general may also be attributed for the fine crystallite size of Chromium obtained by the deposition (Table 4.1 and 4.2)

4.3.2 Wear study

Figure 4.7 shows the variation of cumulative wear loss (in terms of vertical penetration of the indenter or wear of depth) as a function of time of different plating parameter at an applied load of 20 N at 10 rpm sliding speed on a 4 mm diameter track for 15 minutes duration on the coatings.

The wear loss behavior of the coatings developed at different frequency and dutycycle follows the general trend i.e wear loss decreases with increase in frequency and duty cycle. From the Figure 4.7 it can also observed that the wear loss without pulse deposition is higher than the PED samples and also the loss is high for coating developed at 4 kHz and 10 dutycycle than the coating developed at 12 kHz and 8 kHz which has shown increased intensity of (210) line corresponds to (200) (soft mode).

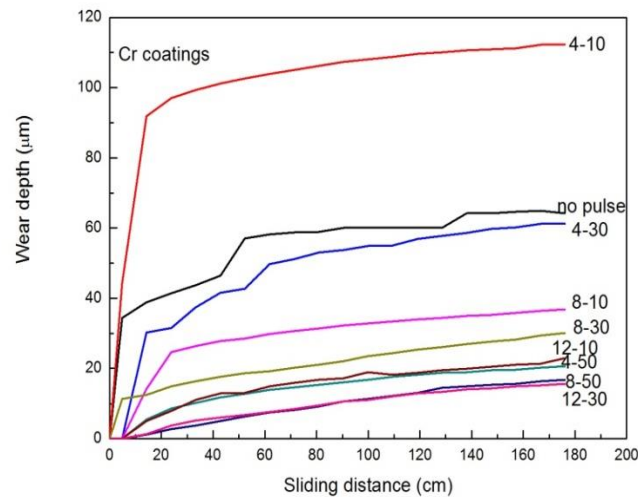
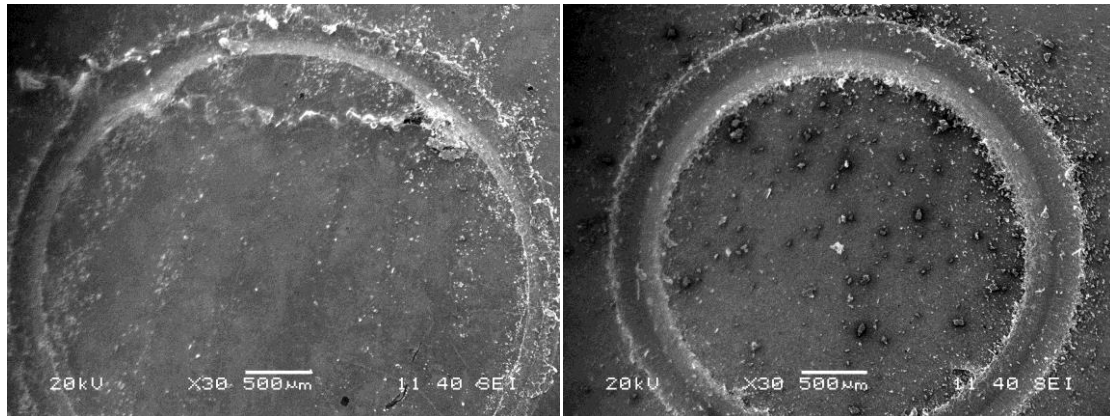


Figure 4.7. Variation of cumulative depth of wear as a function of sliding distance for the Cr coatings at different plating parameters.

In case of some graphs momentary negative slope could be observed. This may due to cold welding of chromium with the hardened diamond ball (indenter) resulting in decrease in the

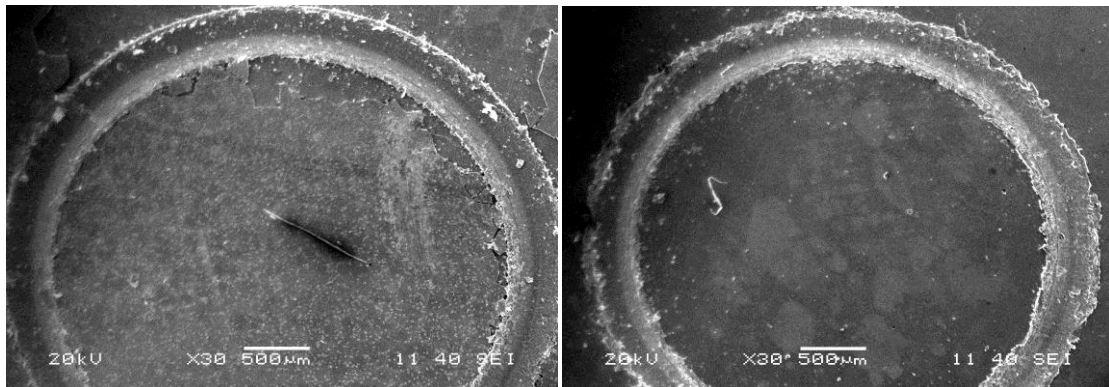
wear depth. In general it be concluded that, with increased frequency the wear depth decreases.

Figure 4.8 shows the SEM micrographs of the worn surfaces of wear tested samples. Figure (a), (b), (c) and (d) shows the overall wear track of the worn wear surfaces whereas Figure (d), (e), (f) & (g) shows the same wear track at higher magnification of pure Cr without pulse, frequency 4 kHz, 8 kHz, 12 kHz.



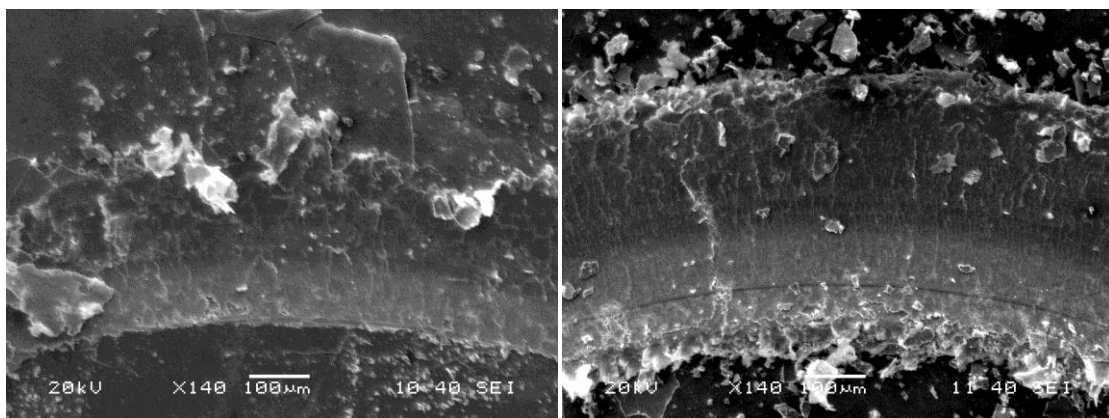
(a)

(b)



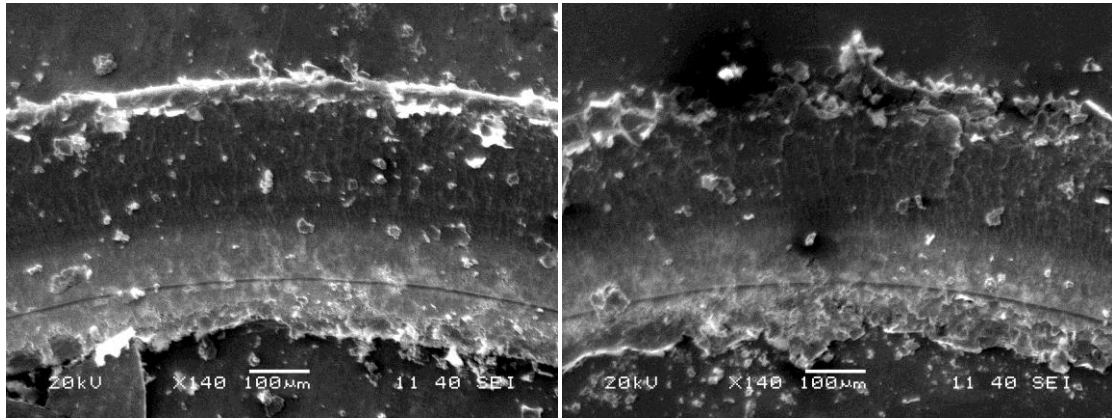
(c)

(d)



(e)

(f)



(g)

(h)

Figure.4.8. Wear track of Cr coating (a) without pulse, (b) frequency 4 kHz (c) frequency 8 kHz (d) frequency 12 kHz at 50 dutycycle respectively and corresponding enlarged view in (e), (f), (g) & (h) respectively

From the figure it can be seen that in case of sample coated with 4 kHz frequency, the wear track width is huge and also the track is not smooth. Narrow wear track width was observed for Cr coating with higher frequency. The sample without pulse has abrasive wear appearance with some cracks at the side of the track whereas adhesive nature of wear can be seen in the other sample of PED deposition.

CHAPTER 5

RESULTS AND DISCUSSIONS OF CHROMIUM-ZIRCONIA COATING

Particle size

Zeta potential measurement

XRD analysis

Microstructural characterization

Surface Mechanical properties

CHAPTER 5

RESULTS AND DISCUSSIONS OF CHROMIUM-ZIRCONIA COATING

5.1 Particle Size:

The Figure 5.1 below shows the particle size distributions of ZrO_2 powder obtained by using Malvern Zeta sizer. From the figure it can be seen that no sharp peak was observed, it indicates that a range of different sized particles were present in the bulk powder. shows the particle size distribution of the ZrO_2 powder and it exhibits only one pack at ~ 940 nm ZrO_2 shows larger particle size and single peak of distribution.

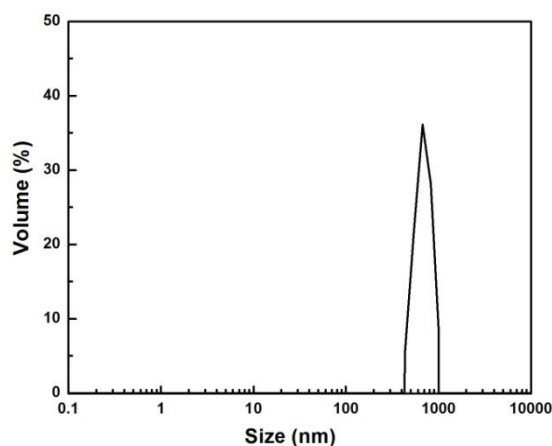


Figure 5.1: Particle size distribution of (a) ZrO_2 powder.

5.2 Zeta potential Measurement:

Zeta potential of ZrO_2 ultrafine particles in de-ionized water at different pH values was measured to determine the iso-electric point for stable suspension by using Malvern Zetasizer nano series Nano- ZS model instrument prior to the electrodeposition. From the below Figure 5.2 it can be observed that the iso-electric point of ZrO_2 was around 5.35 in pH . The pH maintained in our case for Cr- ZrO_2 system was around 1.14, which was lower than the obtained iso-electric point pH , which signifies the acidic nature of the solution and the particles were positively charged in the suspension.

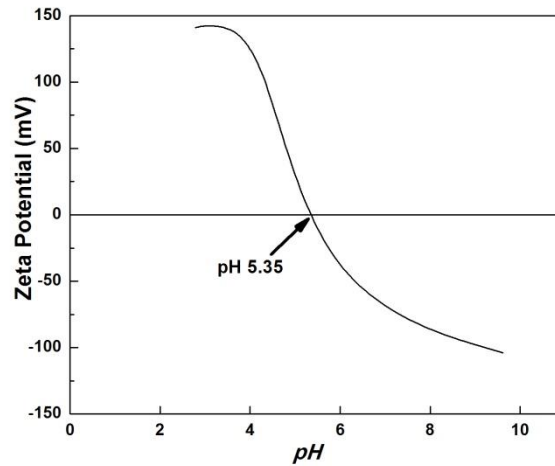


Figure 5.2: *pH* Vs Zeta potential for Iso-electric point determination of (a) ZrO₂.

5.3 XRD Analysis:

The XRD patterns of Cr-ZrO₂ composite coatings prepared at different pulse frequency and duty cycle are illustrated in Figure 5.3. As can be seen from Figure 5.3 (a), the composite coatings exhibit body-centred cubic (bcc) lattice with different orientation which was influenced by the pulse frequency. It can be clearly observed that in the composite coating the diffraction intensity of the (220) orientation increased with the increase of pulse frequency and then decreases. In the four co-deposited samples no significant ZrO₂ peaks were seen, so to study it properly, XRD profile of ZrO₂ was enlarged to see the low intensity peaks in figure 5.3.(c). The texture coefficient of the composite coatings is also influenced by the pulse frequency as seen in Table 5.3. Texture coefficient (TC) of each plane for all the samples were calculated using the following equation:

$$TC(hkl) = \frac{I_{(hkl)}/I_{0(hkl)}}{\sum\{(I_{(hkl)}/I_{0(hkl)})\}} \times 100\%$$

Where $I_{(hkl)}$ is the relative intensity of sample and $I_{0(hkl)}$ is the standard intensity of the oriented sample.

From the Table 5.1 & Figure 5.3 (a) it can be observed that (220) is the most intense diffraction line (texture) in Cr-ZrO₂ composite coatings at 4 kHz frequency. The quality of the (220) texture was obviously affected by the incorporation of particles and the frequency. At both cases (i.e. 8 kHz and 12 kHz) the intensity of (220) is less (1% & 2%) which is accompanied by increase in the intensities of (310) and (420) lines. As the frequency increased from 4 kHz to 8, 12 kHz the intensity of (220) texture increased by 1% and

decrease by 5% respectively, the increase was accompanied by decrease in the intensities of (420) lines, this is due to lower content of ZrO_2 or due to higher over potential which affects the nucleation and growth of crystallites.

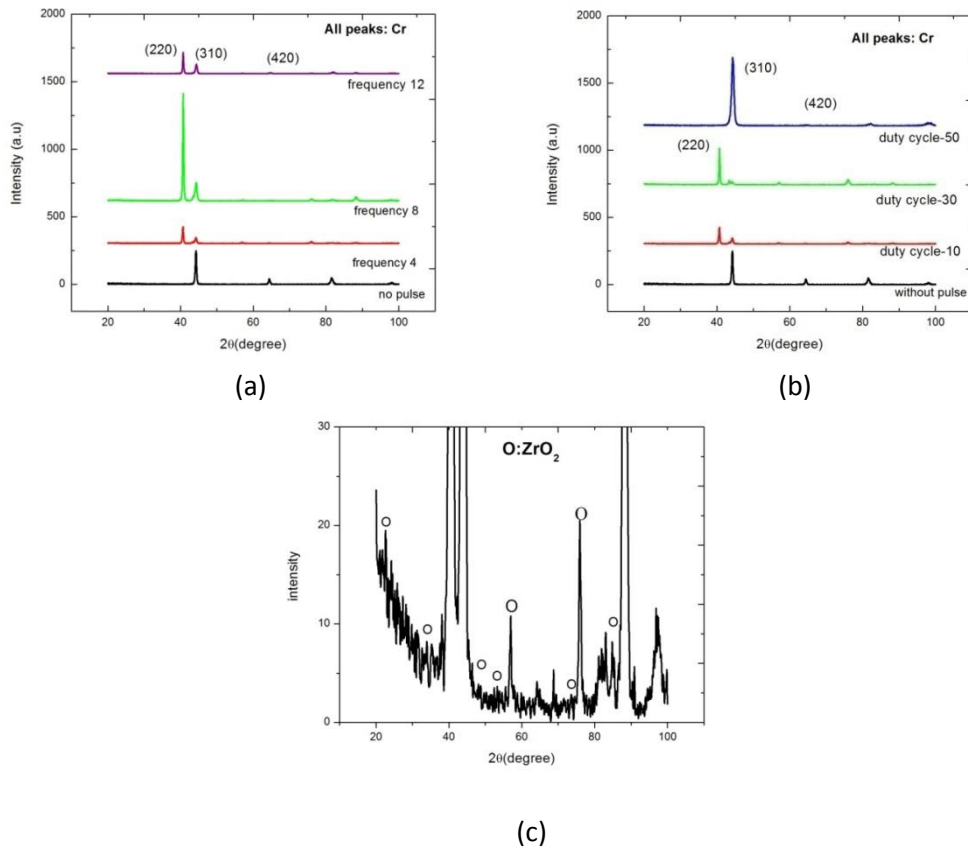


Figure.5.3.(a) XRD pattern of Cr-ZrO₂ at different frequencies(4,8,12)kHz.(b) XRD pattern of Cr-ZrO₂ at different Duty cycle(10,30,50)%.(c) Enlargement of ZrO₂ peaks(8kHz frequency and 30% Duty cycle).

Table 5.1:Effect of different frequencies on texture coefficient of Cr-ZrO₂ composite coating.

Cr-ZrO ₂ Coating/sample	Texture coefficient			Crystallite size (nm)
	(220)	(310)	(420)	
Without pulse	0.00	0.82	0.18	36
4-10	0.77	0.22	0.01	47
8-10	0.76	0.24	0.00	21
12-10	0.74	0.24	0.03	32

Table 5.2:Effect of different duty cycle on texture coefficient of Cr-ZrO₂ composite coating.

Cr-ZrO ₂ Coating/sample	Texture coefficient			Crystalite size (nm)
	(220)	(310)	(420)	
Without pulse	0.00	0.82	0.18	36
4-10	0.77	0.22	0.01	47
4-30	0.96	0.04	0.00	21
4-50	0.00	0.99	0.01	12

From the Table 5.2 & Figure 5.3 (b) it can be observed that (220) is the most intense diffraction line (texture) in Cr-ZrO₂ composite coatings at 30 % duty cycle. At both cases (i.e.10 % and 50 %) the intensity of (220) is less (19% and 96%) which is accompanied by increase in the intensities of (310) and (420) lines. In without pulse samples the most pronounced diffraction line is (310).

In the summary from the above discussions on texture study of Cr-ZrO₂ systems it can be conclude that the observed texture is due to the influence of frequency, duty cycle, embedding second phase ceramic particles in the composite coatings.

In Table 5.1 and 5.2 it can be observed that in general the crystallite size of Chromium coating is fine in nature as calculated from Scherrer equation.

5.4 Microstructure Characterization:

The surface morphology and particle distribution of the electrodeposited composite coatings were performed by using SEM (JEOL JSM-6480LV) and Field Effect Scanning Electron Microscope (FESEM) of ZEISS: SUPRA 40. The below Figure 5.4 shows SEM surface micrographs of the electrodeposited Cr-ZrO₂ composite coatings prepared at frequency 4 kHz, 8 kHz, 12 kHz and at duty cycle of 10, 30, 50 without adding any surfactant to the bath.

From the micrographs a smooth coating can be observed at all deposition condition with no cracks. But still the frequency has a great influence on the structure of the chromium matrix. At 4 kHz, 8 kHz and 12 kHz (Figure 5.4.(a),(b),(c) & (d)) the micrographs were smooth and fully compacted, but small micro pits were observed at 12 kHz frequency this may be is attributed to evolution of hydrogen. The dispersion of nano- ZrO₂ particles in a Cr matrix for

the coating that prepared at duty cycle of 30% is illustrated in Figure 5.5 (b); (c) implies that Chromium and Zirconia particles were uniformly incorporated in the coating.

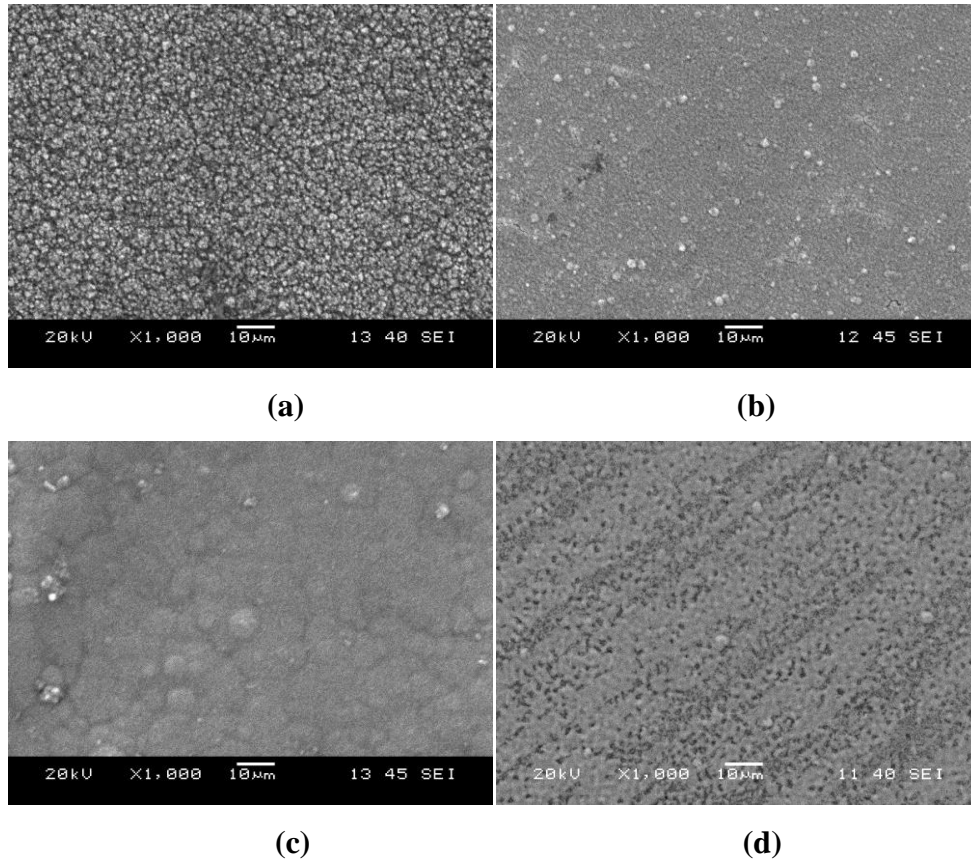
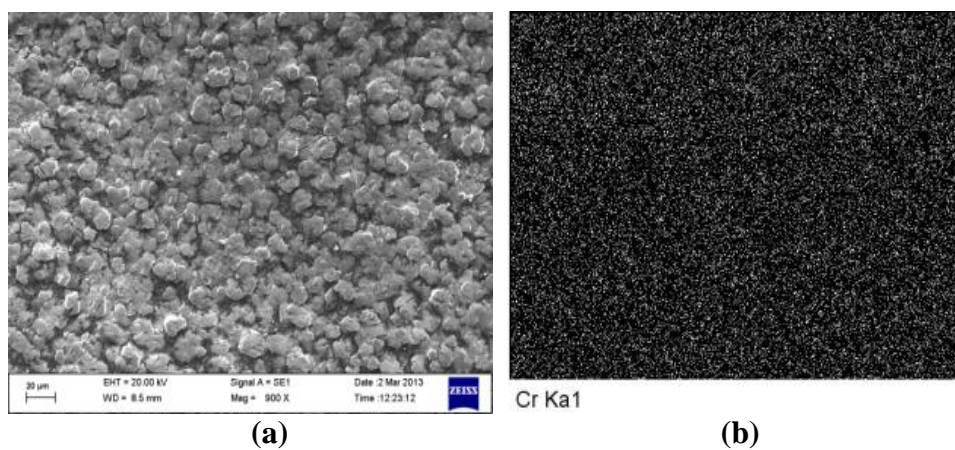
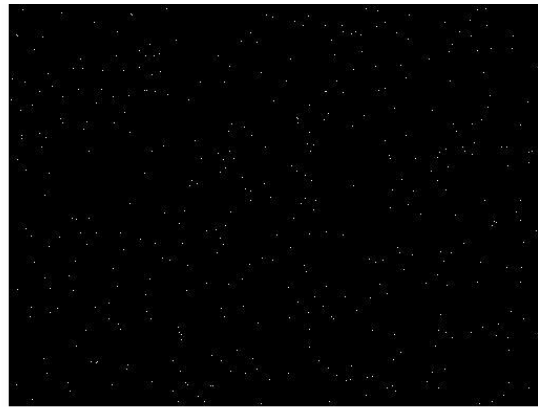


Figure.5.4. SEM image of surface morphology of Cr-ZrO₂ Nano-composite coatings at different pulse frequency: (a) no pulse (b) 4 kHz (c) 8 kHz (d) 12 kHz, duty cycle = 50%.





Zr La1

(c)

Figure.5.5. (a) SEM image of the surface and The corresponding (b) Cr mapping image (c) Zr mapping image, of a Cr-ZrO₂ composite coating produced at frequency of 8 kHz and duty cycle of 30%.

5.5 Microhardness study:

The hardness values were observed are mainly depending on dispersion strengthening due to the dispersed second phase particles and preferred crystal orientation (Texture) of the matrix phase and marginal effect of grain size. Figure 5.6 shows the variation of microhardness values measured on the coated surface as a function of different pulse parameter such as (Frequency, Duty cycle). The microhardness of the composite coatings were measured by using Leco LM700 microhardness tester by applying 50 gf load for 15 seconds in order to ensure that the microhardness values are not affected by the substrate. Figures 5.6 shows the effect of frequency and dutycycle on microhardness of Cr-ZrO₂ composite coatings developed at 4 kHz, 8 kHz, 12 kHz without addition of any surfactant and additives to the bath. Generally the strengthening mechanism of poly crystalline metals, alloys and MMCs mainly due to (a) grain refinement strengthening from Hall-Petch relationship (b) dispersion strengthening due to Orowan mechanism (c) solid solution strengthening (d) crystal orientation. In the present work the hardness values were observed are mainly depending on dispersion strengthening due to the dispersed second phase particles and preferred crystal orientation (Texture) of the matrix phase and marginal effect of grain size.

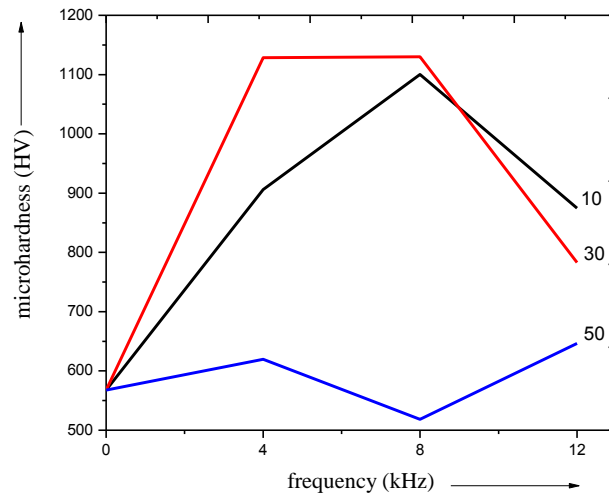


Figure 5.6. (a) Effect of pulse frequency and dutycycle on the hardness of Cr-ZrO₂ composite coatings

The hardness values obtained for the Cr-ZrO₂ composite coating are higher than pure chromium; this is attributed to the dispersion strengthening caused by the dispersed second phase particles in the composite coatings.

When the frequency increased from 0 (i.e. no pulse) to 4 kHz, the hardness values increased and at 12 kHz a little decrease in hardness values were obtained. In case of Cr-ZrO₂ coatings at 12 kHz in all the cases 10, 30, 50 dutycycle less hardness values were reported which is due to the random crystalline orientation (Table 5.1 & 5.2) which leads to decrease in the intensity of (220) texture, and increase in intensity of (420) plane this may be co related with [100] texture associated to deposits with minimum hardness and maximum ductility [88]. The minimum hardness for (310) diffraction line is attributed to lower angle between (310) and (100) planes, which leads to lower strain energy, the strain energy increases as the angle increases [89-90]. At 30 and 50 dutycycle the hardness value obtained was less compare to 10 dutycycle, this is due to the increased intensity of (310) soft mode, increase in grain size and microstructure of the chromium matrix. The higher intensity of (220) plane leads to higher hardness this is due to its less active slip systems [91].

Moreover the higher hardness values in general may also be attributed for the fine crystallite size of Chromium obtained by the deposition (Table 45.1 and 5.2)

5.6 wear study:

The wear test on the surfaces of the composite coatings were carried out by using DUCOM TR-208-M1 ball on plate wear tester by applying load 20 N for 15minutes with 10 rpm

sliding speed on a 4 mm diameter track. The below Figure 5.7 shows the comparable wear loss graphs (in terms of vertical penetration of the indenter or wear depth) as a function of sliding distance of at frequency 4 kHz, 8 kHz, 12 kHz and at duty cycle of 10, 30, 50.

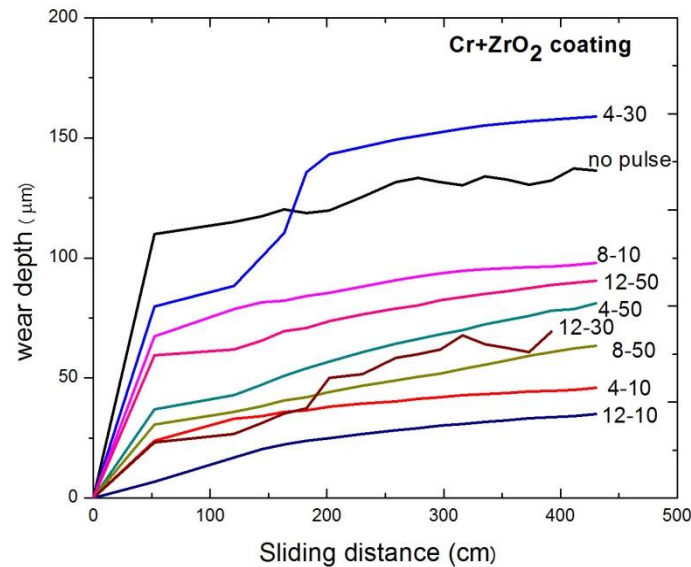
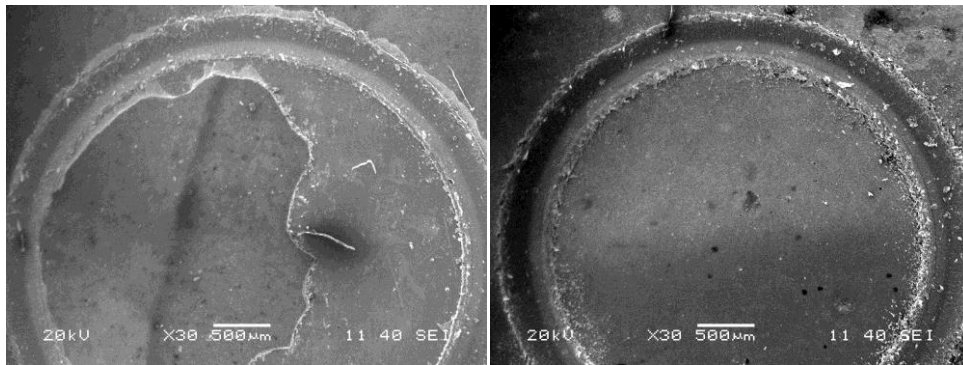


Figure 5.7. Wear depth versus sliding distance plots of Cr-ZrO₂ coatings with different frequencies (4 kHz, 8 kHz, 12 kHz) & different dutycycles (10%, 30%, 50%).

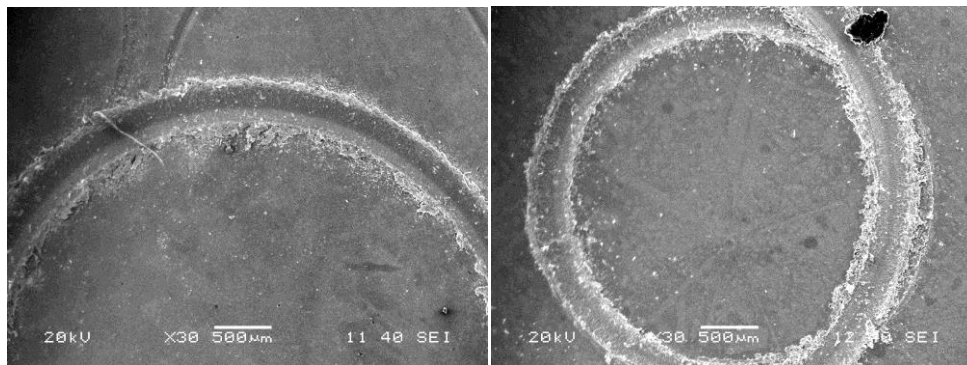
The wear loss behaviour of the coatings developed at different frequency and dutycycle follows the general trend i.e wear loss decreases with increase in frequency and dutycycle. In case of some graphs momentary negative slope could be observed. This may due to cold welding of chromium with the hardened diamond ball (indenter) resulting in decrease in the wear depth. In general it be concluded that, with increase frequency the wear depth decreases. The wear performance of electroplated composite films is known to be mainly dependent on the microstructure of the metal matrix as well as on the amount and distribution of incorporated particles [92-93]. That is the wear behaviour is co related to the hardness of the surface. According to the above statement the wear loss or extent should be high for pure Cr (without oxide particles), and also for lower wt% ZrO₂ embedded samples. From the Figure 5.7 it can also observed that the wear loss of without pulse deposition is higher than the PED samples and also the loss is high for coating developed at 4 kHz and 30 dutycycle than the coating developed at 12 kHz and 8 kHz which has shown increased intensity of (220) line corresponds to (310) (soft mode). This can be attributed to the inherent ductility and softness of the Cr. Figure 5.8 shows the SEM micrographs of the worn surfaces of wear tested samples. Figure (a), (b), (c) and (d) shows the overall wear track of the worn wear surfaces

where as Figure (d), (e), (f) & (g) shows the same wear track at higher magnification of pure Cr-ZrO₂ without pulse, frequency 4 kHz, 8 kHz, 12 kHz.



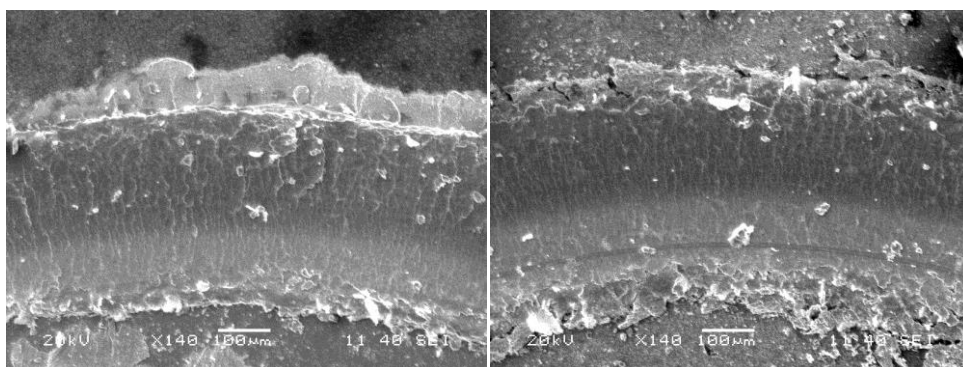
(a)

(b)



(c)

(d)



(e)

(f)

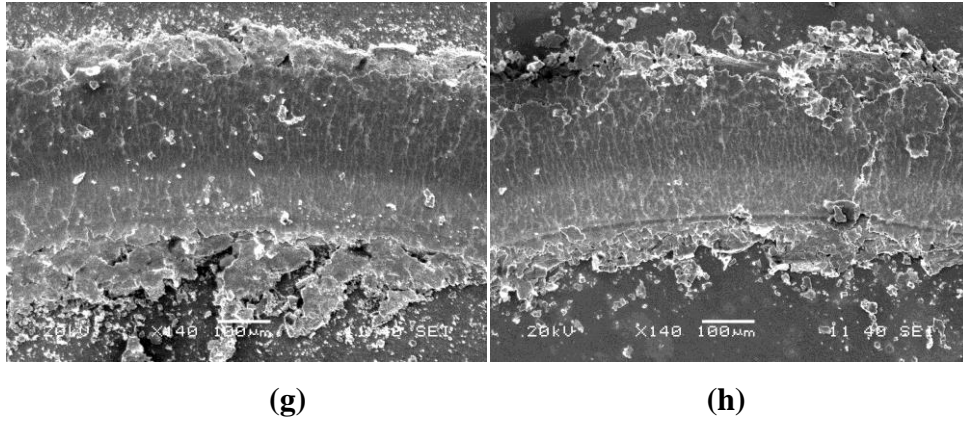


Figure 5.8. Wear track of Cr–ZrO₂ coating (a) without pulse, (b) frequency 4kHz (c) frequency 8kHz(d) frequency 12kHz and corresponding enlarged view in (e) ,(f),(g) and(h) respectively.

Figure 5.8 shows the SEM micrographs of the worn surfaces of wear tested samples. Figure (a), (b), (c) and (d) shows the overall wear track of the worn wear surfaces where as Figure (d), (e), (f) & (g) shows the same wear track at higher magnification of pure Cr-ZrO₂ without pulse, frequency 4 kHz, 8 kHz, 12 kHz. From the figure it can be seen that in case of sample coated with 4 kHz frequency, the wear track width is huge and also the track is not smooth. Slight less wear track width was observed for Cr-ZrO₂ coating with higher frequency. The sample without pulse shows abrasive type of wear with some cracks at the side of the track whereas adhesive kind of wear can be seen in the other sample of PED deposition.

CHAPTER 6

CONCLUSIONS

Conclusions

Scope of future work

6.1 Conclusions

In the present study pure Cr / Cr-ZrO₂ nanocomposite coatings were developed successfully by using Pulse Electrodeposition (PED) process on the mild steel substrate. From the detailed investigation of the results obtained, the following conclusions can be drawn:

- Chromium coating on mild steel substrate were successfully deposited by electro deposition from standard bath with varying pulsed DC parameters.
- From the Texture calculations of Cr in pure Cr coating by PED technique a strong (220) texture was obtained, the intensity of (220) texture and shift of this texture plane to mixed plane orientations was obtained due to the particle incorporation, frequency and dutycycle.
- In pure Cr deposition for any particular frequency, with increase in duty cycle TC (200) increases with decrease in TC (210) and TC (310). Thus as duty cycle increases the preferred orientation tends to be corresponding to the plane of higher strain energy.
- The crystallite size was calculated by using Scherrer formula was below 100 nm for all the coated samples.
- In pure Cr deposition the hardness was higher for deposit corresponding to finer grain sizes and also in case of preferred orientation being on the plane of higher strain energy (here in case of Cr this plane being (210)). Also the hardness values do not differ significantly with grain size, because variation in grain size itself is not any significant.
- In pure Cr deposition Ex-situ SEM images confirm the observation that fine grain size and harder deposition were obtained in case of higher frequency and lower duty cycle (8 kHz and 30% duty cycle).
- The particle size and zeta potential of ZrO₂ were determined by using Zetasizer and the particle size obtained was ~ 900 nm respectively. And the iso electric points were around 5.35 *pH* for ZrO₂.
- The XRD pattern of Cr-ZrO₂ composite coatings does not ZrO₂ show peaks clearly with much intensity because of less wt% (less than 10%) of powders embedded in the composite coatings.

- A smooth, no dendrites, cracks and nodule like structures were observed on the surfaces. In case of Cr-ZrO₂ coatings at higher frequency (12 kHz) the coatings were fully compacted.
- The microhardness values obtained for the composite coatings are higher than the pure Cr coating hardness, the improvement is attributed to dispersion strengthening caused by the embedded second phase particles, texture and modified microstructure of chromium matrix.
- The wear resistance of the composite coatings with PED was higher than conventional DC technique. The wear loss behaviour of the coatings developed at different frequency and dutycycle follows the general trend i.e wear loss decreases with increase in frequency and duty cycle The addition of ceramic oxide particles marginally transforms the wear from adhesive (unreinforced chromium) to abrasive type.

CHAPTER 7

REFERENCES

CHAPTER 7

REFERENCES

1. U. Erb: *Nanostruct. Mater.*, 1995, Vol. 6.

2. D.Clark, D.Wood, U.Erb: *Nanostruct. Mater.*, 1997, Vol. 9.
3. A.Robertson, U.Erb, G.Palumbo: *Nanostruct. Mater.*, 1999, Vol. 12.
4. A.M. Rashidi, A.Amadeh: *J. Mater. Sci. Eng.*, 2010, Vol. 26.
5. P.M. Vereecken, I.Shao, P.C. Searson: *J. Electrochem. Soc.*, 2000, Vol. 147.
6. J.L.Stojak, J.Fransaer, J.B.Talbot, R.C. Alkire, D.M. Kolb: *Adv. Electrochem. Eng.*, 2002, Vol. 7.
7. A.Hovestad, L.J.J. Janssen: *J. Appl. Electrochem.*, 1995, Vol. 25.
8. C.U. Chisholm: *Electrodeposition. Surf. Treat*, 1975, Vol. 3.
9. S. Surviliene: *Surf. Coat. Technol.*, 2001, Vol. 137.
10. Zhixiang Zeng, Junyan Zhang : *Wear* 1996, Vol. 52.
11. Bin liu, Zhixiang Zeng, Yimin Lin: *Surf. Coat. Technol.*, 2009, Vol. 13.
12. Jifeng Gao, Jinping Suo: *Appl. Surf. Sci.* 2011, Vol. 202.
13. M. Rezaei-Sameti, S.Nadali, J.Rajabi, M.Rakhshi: *J. Mol. Struc.*, 2012, Vol. 1020.
14. E. Budevski, G. Staikov, W.J. Lorenz, *Electrochemical Phase Formation and Growth*, VCH, Weinheim, 1996.
15. J.C. Puipe, *Schriftenreihe Galvanotechnik: Pulse-Plating*, Leuze Verlag, Bad Saulgau, 1986.
16. A.F. Zimmerman, D.G. Clark, K.T. Aust, U. Erb: *Mater. Lett.*, 2002, Vol. 52 .
17. C. Kollia, Z. Loizos, N. Spyrellis: *Surf. Coat. Technol.*, 1991, Vol. 45.
18. P.T.Tang, P.Watanabe, J.E.T. Andersen, G. Bech-Nielsen: *J. Appl. Electrochem.* 1995, Vol. 25.
19. R. Mishra, R. Balasubramaniam: *Corros. Sci.* 2004, Vol. 46.
20. C.Y. Dai, Y. Pan, S. Jiang, Y.C. Zhou: *Surf. Rev. Lett.* 2004 , Vol 11.
21. S. Tao, D.Y. Li: *Nanotechnology*, 2006, Vol 17.
22. R.Chattopadhyay —*Advanced Thermally Assisted Surface Engineering Processes* Kluwer Academic Publishers, MA, USA (now Springer, NY), 2004
23. S.Frainger, Blunt: *J. Eng. Coat. Des. App.*, 2nd edition, Abington Publishing, Abington, England, 1998.
24. A.Brenner, and Riddell. G, *Deposition from Aqueous solution: An overview*, *J. Res. Natl.*, Bureau of Standards, 1947, Vol. 39
25. C.C.Koch: *Nano structure materials: Processing, Properties and Potential Applications*, Noyes Publications, New York, 2002, Vol. 612.

26. M.J.N.V Prasad, P.Ghosh, A.H.Chokshi: *Journal of the Indian Institute of Science*, 2009 Vol. 89.
27. H.Natter and R.Hempelmann : *J. Phys. Chem.*, 1996,vol 17.
28. Vijendra Singh, Physical Metallurgy, Lomus Offset Press, Delhi, 1999.
29. P.B.S.N.V.Prasad, R.Vasudevan S.K.Seshadri and S.Ahila: *Mater .Lett.*, 1993, vol,17.
30. Fan chonglun, D. L Piron: *Electrochimi. Acta.*, 1996, Vol. 41.
31. M. Uhlemann, A. Gebert, M. Herrich, A.Krause, A.Cziraki, Schultz : *Electrochimi. Acta.*, 2003,Vol,48.
32. M.C.Rastogi, Surface and interfacial science, Narosa publishing house, 2003
33. Matthias Seiler, “Hyperbranched polymers: Phase behavior and new applications in the field of chemical engineering”, *Fluid Phase Equilibria*, 2006, Vol. 241.
34. Wang Zhen-Gang, Wan Ling-Shu and Xu Zhi-Kang, “Surface engineerings of polyacrylonitrile-based asymmetric membranes towards biomedical applications: An overview”, 2007, Vol. 304.
35. Haijun Zhao, Lei Liu, Wenbin Hu and Bin Shen: *Mater. Des.*, 2007,Vol . 28.
36. Ming-Der Ger, Bing Joe Hwang: *Mater. Chem. Phys.*, 2002 Vol. 76.
37. G. Dubpernell: *Plating.*, 1960, Vol. 47.
38. C. G. Fink,U.S. Patents 1,581,188 (1926), Vol.463
39. Elektro-Chrom-G.m.b.H. (assignee of E. Leibreich), German Patent 448,526 (1927); British Patent 237,288 (1925); French Patent 601,059 (1926); Swiss Patent 118,632 (1927).
40. Fei Luo, Xiaolu Pang, Kewei Gao, Huisheng Yang, Yanbin Wang, *Surf. Coat.Technol*, 2007,Vol 202.
41. Aimin Liang, Liwei Ni, Qiao Liu, Junyan Zhang: *Surf .coat. Technol.*, 2013, Vol 218.
42. Hanzhuo Zhang, Zhonghao Jiang, Yinghuai Qiang: *Mater. Sci. Eng* 2009,Vol. 517.
43. C.Shanthi, S.Barathan, Rajasrisen Jaiswal, R.M Arunachalam, S.Mohan: *Mater. Lett.* 2008, Vol. 62.
44. Xi Zhang, K. N. Tu, Zhong Chen, Y. K. Tan, C. C. Wong: *J. Nano .sci. Nanotechno.*, 2008, vol.8.
45. Wonbaek kim and Rolf well: *Surf .Coat. Technol.*, 1989, Vol 38.
46. R.Gyana, K. Pattanaik, Dinesh, Pandya and Subhash C. Kashyap: *J. Electrochem. Soc.*, 2002, vol 149.
47. Watanabe Tohru, Nano plating-Microstructure control theory of plated film and data base of plated film microstructure, Elsevier Ltd, 2004.

48. M.Schario Troubleshooting decorative nickel plating solutions (Part I of III installments): *Metal Finishing*, 2007, Vol. 105.
49. J.L.Stojak, J.Fransaer, J.B.Talbot, in: R.C. Alkire, D.M. Kolb. *Adv. Electrochem Sci. Eng.*, Wiley-VCH, Weinheim, 2002, vol. 7.
50. A. Bund, D. Thiemig: *J. Appl. Electrochem.* 2007, Vol. 37.
51. I. Garcia, J. Fransaer, J.P. Celis: *Surf. Coat. Technol.* 2001, Vol.137.
52. S.C. Wang, W.C. Wei: *J.Mater. Chem .Phys.* 2003, Vol. 574.
53. M. Kaisheva, J. Fransaer: *J. Electrochem. Soc.* 2004, Vol.151.
54. E.A. Pavlatou, M. Stroumbouli, P. Gyftou, N. Spyrellis: *J. Appl .Electrochem.* 2006, Vol. 36 .
55. Kelly J.J, P.E.Braddey , Landolt. D: *Electrochem. Acta* 2000, Vol. 147.
56. Furusawa Kunio, Matsumura Hideo, Dekker Encyclopedia of Nanoscience and Nanotechnology, Second Edition, 2009, Vol.131.
57. R.Boccaccini Aldo, Zhitomirsky Igor, Application of electrophoretic and electrolytic deposition techniques in ceramics processing, *Current Opinion in Solid State and Materials Science*, 2002, Vol. 6.
58. Laxmidhar Besra, Meilin Liu: *Prog. Mater. Sci*, 2007, vol 52.
59. K.Hasegawa, S.Kunugi, M.Tatsumisago, T.Minami: *J Sol gel. Sci. Technol*, 1999, Vol. 15.
60. W.Shan, Y.Zhang, W.Yang, C.Ke, Z.Gao, Y.Ke : *Micropor. Mesopor. Mater*, 2004, vol 69.
61. Wei M, Ruys AJ, Milthorpe BK, Sorrell CC, Evans JH: *J Sol gel. Sci. Technol*, 2001, vol 21.
62. TM Sridhar, UK Mudali: *Trans Ind Inst Met*, 2003, vol 56.
63. MJ Shane, JB Talbot, BG Kinney, Sluzky E, Hesse HR.: *J. Colloid.I nterface. Sci*, 1994, vol 165.
64. MJ Shane, JB Talbot, RG Schreiber, CL Ross, Sluzky E, Hesse KR: *J. Colloid Interface. Sci* ,1994, vol.165.
65. Cao, Guozhong, *Nanostructures and Nanomaterials – Synthesis, Properties and Applications*, Imperical College Press, 2004.
66. L Jean. Stojak, Jan Fransaer and Jan B. Talbot: *Adv. Electrochem. Sci. Eng.*, 2001, Vol 7.
67. . L Jean, Stojak and B. Jan. Talbot, *J. Appl .Electrochem.*, vol 31.
68. P.R, Ebdon. *Plat. Surf. Finish*, 1988, vol,75.

69. Lu Xinying, Rizhang Zhu and Yedong He: *Oxid. met*, 1995, vol 43.
70. W.Metzger., Ott. R, Laux. G, et al., Electrodeposition of dispersion hardened nickel, *Galvanoteknik* (in German), 1970, vol, 61.
71. Jianhua Zhu, Lei Liu , Guohua Hu , Bin Shen , Wenbin Hu and Wenjiang Ding, *Mater.Lett*, 2004, vol 58.
72. Lozano-Morales.A and Podlaha. E.J: *J.Electrochem. Soc.*, 2004, vol 151.
73. V .Medelien.: *Surf. Coat. Technol*, 2002,vol 154.
74. J.Steven. Osborne, Wendi S. Sweet, Kenneth S. Vecchio, and Jan B. Talbot, *J. Electrochem. Soc.*, 2007, Vol 154.
75. Bharat.Bhusan, B.K.Gupta, Michael H. Azarian: *Wear.*, 1995, vol 181.
76. M. Scholl, R. Devanathan, P. Clayton, 1990, Vol 135.
77. D.Z. Guo, L.J.Wang, J.Z. Li, *Wear*, 1993, vol 161.
78. G.E.D'Errico, S Bugliosi, R Calzavarini, D. Cuppini, *Wear*, 1999, vol 225–229.
79. S. Ramalingam, V.S Muralidharan. and Subramania. A: *J. Solid. State. Electrochem.*, 2009, vol.13.
80. Andreas Bund and Denny Thiemig, 2007, vol, 37.
81. www.dynacer.com
82. www.obz-innovation.de
83. D.Kennedy, Xue, Y., Mihaylova, M. *The Engineers Journal (Technical)* 2005, vol.59.
84. www.silver-colloids.com
85. depts..washington.edu
86. L. Chen, L. Wang, Z. Zeng, T. Xu: *Surf. Coat. Technol.* 2006, vol.201.
87. Abdel Aal. A, Hassan. H.B: *J. Alloys. Compd.*, 2009, vol 477.
88. Lajevardi. S.A, Shahrabi. T: *Appl. Surf. Sci*, 2010, vol 256.
89. DhananjayKumar Singh and V. B. Singh, *J. Electrochem. Soc.*, 2011, vol 158.
90. Jian-Min Zhang: *Mater. Lett.*, 2008, vol 62.
91. Jian Feng Wang: *Adv. Mater.*, 2010, vol 609.
92. Vipin chawla, Jayaganthan R and Ramesh Chandra: *Mater. Sci*, 2009, vol. 32.
93. K.H .Hou, Ger. M.D, Wang. L.M, Ke. S.T: *Wear* 2002, vol.253.
94. S.T Aruna, V.K.William Grips, K.S.Rajam,: *J. Alloys. Compd* 2009, vol.468